5

ANALYSIS OF SECTIONS FOR FLEXURE

5-1 Introduction and Sign Conventions

Differentiation can be made between the *analysis* and *design* of prestressed sections for flexure. By *analysis* is meant the determination of stresses in the steel and concrete when the form and size of a section are already given or assumed. This is obviously a simpler operation than the *design* of the section, which involves the choice of a suitable section out of many possible shapes and dimensions. In actual practice, it is often necessary to first perform the process of design when assuming a section, and then to analyze that assumed section. But, for the purpose of study, it is easier to learn first the methods of analysis and then those of design. This reversal of order is desirable in the study of prestressed as well as reinforced concrete.

This chapter will be devoted to the first part, the analysis; the next chapter will deal with *design*. The discussion is limited to the analysis of sections for flexure, meaning members under bending, such as beams and slabs. Only the effect of moment is considered here; that of shear and bond is treated in Chapter 7.

A rather controversial point in the analysis of prestressed-concrete beams has been the choice of a proper system of sign conventions. Many authors have used positive sign (+) for compressive stresses and negative sign (−) for tensile stresses, basing their convention on the idea that prestressed-concrete beams are normally under compression and hence the plus sign should be employed to denote that state of stress. The author prefers to maintain the common sign convention as used for the design of other structures; that is, minus for compressive and plus for tensile stresses. Throughout this treatise, plus will stand for tension and minus for compression, whether we are talking of stresses in steel or concrete, prestressed or reinforced. When the sense of the stress is self-evident, signs will be omitted.

5-2 Stresses in Concrete Due to Prestress

Some of the basic principles of stress computation for prestressed concrete have already been mentioned in section 1-2. They will be discussed in greater detail here. First of all, let us consider the effect of prestress. According to present

practice, stresses in concrete due to prestress are always computed by the elastic theory. Consider the prestress F existing at the time under discussion, whether it be the initial or the final value. If F is applied at the centroid of the concrete section, and if the section under consideration is sufficiently far from the point of application of the prestress, then, by St. Venant's principle, the unit stress in concrete is uniform across that section and is given by the usual formula,

$$f=\frac{F}{A}$$

where A is the area of that concrete section.

For a pretensioned member, when the prestress in the steel is transferred from the bulkheads to the concrete, Fig. 5-1, the force that was resisted by the bulkheads is now transferred to both the steel and the concrete in the member. The release of the resistance from the bulkheads is equivalent to the application of an opposite force F_i to the member. Using the transformed section method, and with A_c = net sectional area of concrete, the compressive stress produced in the concrete is

$$f_c=\frac{F_i}{A_c+nA_s}=\frac{F_i}{A_t} \tag{5-1}$$

while that induced in the steel is

$$\Delta f_s=nf_c=\frac{nF_i}{A_c+nA_s}=\frac{nF_i}{A_t} \tag{5-2}$$

which represents the immediate reduction of the prestress in the steel as a result of the transfer.

Although this method of computation is correct according to the elastic theory, the usual practice is not to follow such a procedure, but rather to consider the prestress in the steel being reduced by a loss resulting from elastic

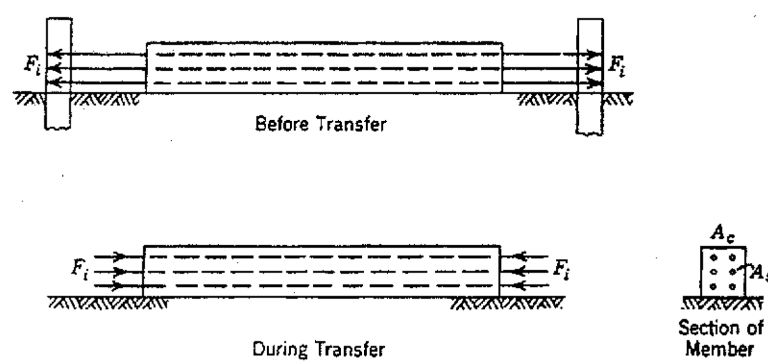

Fig. 5-1. Transfer of concentric prestress in a pretensioned member.

shortening of concrete and approximated by

$$\Delta f_s = \frac{nF_i}{A_c} \quad \text{or} \quad \frac{nF_i}{A_g} \tag{5-3}$$

which differs a little from formula 5-2 but is close enough for all practical purposes, since the total amount of reduction is only about 2 or 3% and the value of n cannot be accurately known anyway. The high-strength steel used for prestressing requires smaller area for the tension steel than would be used in reinforced concrete, thus there is not a large difference between A_c and A_g.

After the transfer of prestress, further losses will occur owing to the creep and shrinkage in concrete. Theoretically, all such losses should be calculated on the basis of a transformed section, taking into consideration the area of steel. But, again, that is seldom done, the practice being simply to allow for the losses by an approximate percentage. In other words, the simple formula $f=F/A$ is always used, with the value of F estimated for the given condition, and the gross area of concrete used for A. For a posttensioned member, the same reasoning holds true. Suppose that there are several tendons in the member prestressed in succession. Every tendon that is tensioned becomes part of the section after it is bonded by grouting. The effect of tensioning any subsequent tendon on the stresses in the previously tensioned ones should be calculated on the basis of a transformed section. Theoretically, there will be a different transformed section after the tensioning of every tendon. However, such refinements are not justified, and the usual procedure is simply to use the formula $f=F/A$, with F based on the initial prestress in the steel.

EXAMPLE 5-1

A pretensioned member, similar to that shown in Fig. 5-1, has a section of 8 in. by 12 in. (203 mm by 305 mm). It is concentrically prestressed with 0.8 sq in. (516 mm^2) of high-tensile steel wire, which is anchored to the bulkheads of a unit stress of 150,000 psi (1034 N/mm^2). Assuming that $n=6$, compute the stresses in the concrete and steel immediately after transfer.

Solution

1. An exact theoretical solution. Using the elastic theory, we have

$$f_c = \frac{F_i}{A_c+nA_s} = \frac{F_i}{A_g+(n-1)A_s}$$

$$= \frac{0.8\times 150{,}000}{12\times 8+5\times 0.8} = 1200 \text{ psi } (8.3 \text{ N/mm}^2)$$

$$nf_c = 6\times 1200 = 7200 \text{ psi } (49.6 \text{ N/mm}^2)$$

Stress in steel after transfer $=150{,}000-7200=142{,}800$ psi (985 N/mm^2).

Solution

2. An approximate solution. The loss of prestress in steel due to elastic shortening of concrete is estimated by

$$= n\frac{F_i}{A_g}$$

$$= 6\frac{120{,}000}{8\times 12} = 7500 \text{ psi } (51.7 \text{ N/mm}^2)$$

Stress in steel after loss $=150{,}000-7500=142{,}500$ psi (983 N/mm^2). Stress in concrete is

$$f_c = \frac{142{,}500\times 0.8}{96} = 1190 \text{ psi } (8.2 \text{ N/mm}^2)$$

Note that, in this second solution, the approximations introduced are: (1) using gross area of concrete instead of net area, (2) using the initial stress in steel instead of the reduced stress. But the answers are very nearly the same for both solutions. The second method is more convenient and is usually followed.

Next, suppose that the prestress F is applied to the concrete section with an eccentricity e, Fig. 5-2; then it is possible to resolve the prestress into two components: a concentric load F through the centroid, and a moment Fe. By the usual elastic theory, the fiber stress at any point due to moment Fe is given by the formula

$$f = \frac{My}{I} = \frac{Fey}{I} \tag{5-4}$$

Then the resultant fiber stress due to the eccentric prestress is given by

$$f = \frac{F}{A} \pm \frac{Fey}{I} \tag{5-5}$$

The question again arises as to what section should be considered when computing the values of e and I, whether the gross or the net concrete section or the transformed section, and what prestress F to be used in the formula, the initial or the reduced value. Consider a pretensioned member, Fig. 5-3. The steel has already been bonded to the concrete; the release of the force from the bulkhead is equivalent to the application of an eccentric force to the composite member; hence the force should be the total F_i, and I should be the moment of

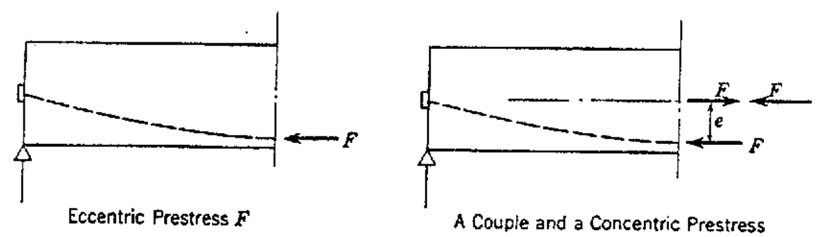

Fig. 5-2. Eccentric prestress on a section

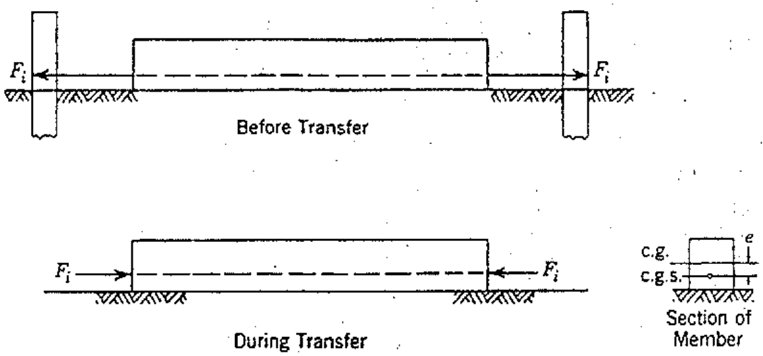

Fig. 5-3. Transfer of eccentric prestress in a pretensioned member.

inertia of the transformed section, and e should be measured from the centroidal axis of that transformed section. However, in practice, this procedure is seldom followed. Instead, the gross or net concrete section is considered, and either the initial or the reduced prestress is applied. The error is negligible in most cases.

EXAMPLE 5-2

A pretensioned member similar to that shown in Fig. 5-3 has a section of 8 in. by 12 in. (203 mm by 305 mm) deep. It is eccentrically prestressed with 0.8 sq in. (516 mm^2) of high-tensile steel wire which is anchored to the bulkheads at a unit stress of 150,000 psi (1034 N/mm^2). The c.g.s. is 4 in. (101.6 mm) above the bottom fiber. Assuming that $n=6$, compute the stresses in the concrete immediately after transfer due to the prestress only.

Solution

1. An exact theoretical solution. Using the elastic theory, the centroid of the transformed section and its moment of inertia are obtained as follows. Referring to Fig. 5-4, for $(n-1)A_s=5\times 0.8=4$ sq in.,

$$y_0=\frac{4\times 2}{96+4}=0.08 \text{ in. } (2.032 \text{ mm})$$

$$I_t=\frac{8\times 12^3}{12}+96\times 0.08^2+4\times 1.92^2$$
$$=1152+0.6+14.7$$
$$=1167.3 \text{ in.}^4\ (485.9\times 10^6 \text{ mm}^4)$$

$$\text{Top fiber stress}=\frac{F_i}{A_t}+\frac{F_i ey}{I_t}$$
$$=\frac{-120{,}000}{100}+\frac{120{,}000\times 1.92\times 6.08}{1167.3}$$
$$=-1200+1200$$
$$=0$$

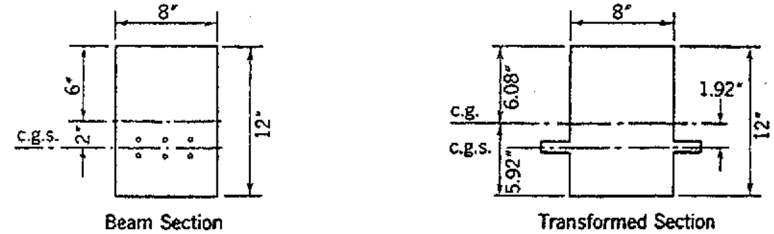

Fig. 5-4. Example 5-2.

$$\text{Bottom fiber stress}=\frac{-120{,}000}{100}-\frac{120{,}000\times 1.92\times 5.92}{1167.3}$$
$$=-1200-1170$$
$$=-2370 \text{ psi } (-16.34 \text{ N/mm}^2)$$

Solution

2. An approximate solution. The loss of prestress can be approximately computed, as in example 5-1, to be 7500 psi in the steel. Hence the reduced prestress is 142,500 psi or 114,000 lb. Extreme fiber stresses in the concrete can be computed to be

$$f_c=\frac{F}{A}\pm\frac{Fey}{I}$$
$$=\frac{-114{,}000}{96}\pm\frac{114{,}000\times 2\times 6}{(8\times 12^3)/12}$$
$$=-1187\pm 1187$$
$$=0 \text{ in the top fiber}$$
$$=-2374 \text{ psi } (-16.37 \text{ N/mm}^2) \text{ in the bottom fiber}$$

The approximations here introduced are: using an approximate value of reduced prestress, and using the gross area of concrete. This second solution, although approximate, is more often used because of its simplicity.

Now consider a pretensioned curved member as in Fig. 5-5. If the transfer of prestress is considered as a force F_i applied at each end, the eccentricity and the

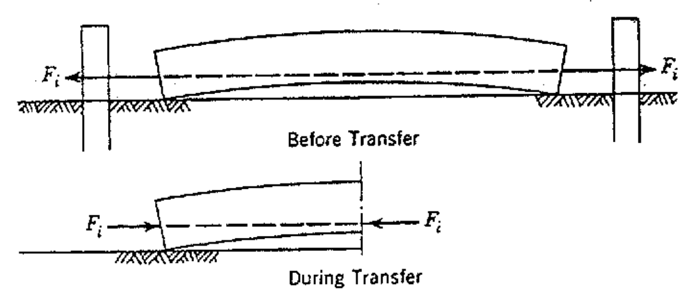

Fig. 5-5. Transfer of prestress in a curved pretensioned member.

moment of inertia will vary for each section. If the exact method of elastic analysis is preferred, different I's and e's will have to be computed for different sections. If an approximate method is permitted, a constant I based on the gross concrete area would suffice for all sections, and the eccentricity can be readily measured from the middepth of the section.

For a posttensioned member before being bonded, the prestress F to be used in the stress computations is again the initial prestress minus the estimated losses. For the value of I, either the net or the gross concrete section is used, although, theoretically, the net section is the correct one. After the steel is bonded to the concrete, any loss that takes place actually happens to the section as a whole. However, for the sake of simplicity, a rigorous analysis based on the transformed section is seldom made. Instead, the reduced prestress is estimated and the stresses in the concrete are computed for that reduced prestress acting on the net concrete section (gross concrete section may sometimes be conveniently used). Stresses produced by external loads, however, are often computed on the basis of the transformed section if accuracy is desired; otherwise, gross section is used for the computation. The permissible simplifications for each case will depend to a large degree on the degree of accuracy required and the time available for computation.

EXAMPLE 5-3

A posttensioned beam has a midspan cross section with a duct of 2 in. by 3 in. (50.8 mm by 76.2 mm) to house the wires, as shown in Fig. 5-6. It is prestressed with 0.8 sq in. (516 mm²) of steel to an initial stress of 150,000 psi (1034 N/mm²). Immediately after transfer the stress is reduced by 5% owing to anchorage loss and elastic shortening of concrete. Compute the stresses in the concrete at transfer.

Solution

1. Using net section of concrete. The centroid and I of the net concrete section are computed as follows

$$A_c = 96 - 6 = 90 \text{ sq in. } (58.1\times 10^3 \text{ mm}^2)$$

$$y_0 = \frac{6\times 3}{96-6} = 0.2 \text{ in. } (5.08 \text{ mm})$$

$$I = \frac{8\times 12^3}{12} + 96\times 0.2^2 - \frac{2\times 3^3}{12} - 6\times 3.2^2$$
$$= 1152 + 3.8 - 4.5 - 61.5$$
$$= 1090$$

Total prestress in steel $= 150{,}000\times 0.8\times 95\% = 114{,}000$ lb (507 kN)

$$f_c = \frac{-114{,}000}{90} \pm \frac{114{,}000\times 3.2\times 5.8}{1090}$$
$$= -1270 + 1940 = +670 \text{ psi } (+4.62 \text{ N/mm}^2) \text{ for top fiber}$$
$$f_c = -1270 - 2070 = -3340 \text{ psi } (-23.03 \text{ N/mm}^2) \text{ for bottom fiber}$$

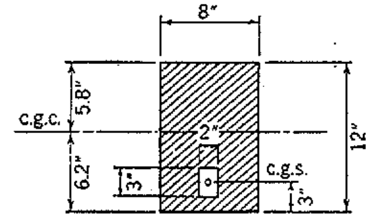

Fig. 5-6. Example 5-3.

Solution

2. Using the gross section of concrete. An approximate solution using the gross concrete section would give results not so close in this case (11% difference):

$$f_c = \frac{-114{,}000}{96} \pm \frac{114{,}000\times 3\times 6}{(8\times 12^3)/12}$$
$$= -1270 + 1940 = +1783$$
$$= +596 \text{ psi } (+4.11 \text{ N/mm}^2) \text{ for top fiber}$$
$$= -2970 \text{ psi } (-20.48 \text{ N/mm}^2) \text{ for bottom fiber}$$

If the eccentricity does not occur along one of the principal axes of the section, it is becessary to further resolve the moment into two component moments along the two principal axes, Fig. 5-7; then the stress at any point is given by

$$f = \frac{F}{A} \pm \frac{Fe_x x}{I_x} \pm \frac{Fe_y y}{I_y}$$

Since concrete is not a really elastic material, the above elastic theory is not exact. But, within working loads, it is considered an accepted form of computation. When the stresses are excessively high, the elastic theory may no longer be nearly correct.

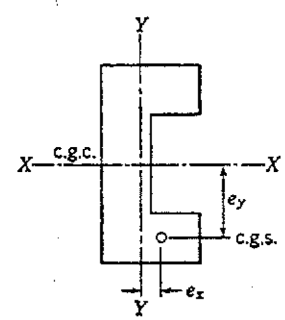

Fig. 5-7. Eccentricity of prestress in two directions.

The above method further assumes that the concrete section has not cracked. If it has, the cracked portion has to be computed or estimated, and computations made accordingly. The computation for cracked section in concrete is always complicated. Fortunately, such a condition is seldom met with in actual design of prestressed concrete. In general, any high-tensile stresses produced by prestress are counterbalanced by compressive stresses due to the weight of the member itself, so that in reality no cracks exist under the combined action of the prestress and the beam's own weight. Hence the entire concrete section can be considered as effective, even though, at certain stages of the computation, high-tensile stresses may appear on paper.

During posttensioning operations, concrete may be subjected to abnormal stresses. Suppose that there is one tendon at each corner of a square concrete section. When all four tendons are tensioned, the entire concrete section will be under uniform compression. But when only one tendon is fully tensioned, there will exist high tensile stress as well as high compressive stress in the concrete. If two jacks are available, it may be desirable to tension two diagonally opposite tendons at the same time. Sometimes it may be necessary to tension the tendons in steps, that is, to tension them only partially and to retension them after others have been tensioned. Computation for stresses during tensioning is also made on the elastic theory. It is believed that the elastic theory is sufficiently accurate up to the point of cracking, although it cannot be used to predict the ultimate strength.

Control of allowable stresses is a means of controlling serviceability, and the ACI Code continues to use limiting values of allowable stresses.

5-3 Stresses in Concrete Due to Loads

Stresses in concrete produced by external bending moment, whether due to the beam's own weight or to any externally applied loads, are computed by the usual elastic theory.

$$f=\frac{My}{I} \tag{5-6}$$

For a pretensioned beam, steel is always bonded to the concrete before any external moment is applied. Hence the section resisting external moment is the combined section. In other words, the values of y and I should be computed on the basis of a transformed section, considering both steel and concrete. For approximation, however, either the gross or the net section of concrete alone can be used in the calculations; the magnitude of error so involved can be estimated and should not be serious except in special cases.

When the beam is posttensioned and bonded, for any load applied after the bonding has taken place, the transformed section should be used as for pretensioned beams. However, if the load or the weight of the beam itself is applied

before bonding takes place, it acts on the net concrete section, which should hence be the basis for stress computation. For posttensioned unbonded beams, the net concrete section is the proper one for all stress computations. It should be borne in mind, though, that when the beam is unbonded, any bending of the beam may change the overall prestress in the steel, the effect of which can be separately computed or estimated as discussed in section 4-5.

Often, only the resulting stresses in concrete due to both prestress and loads are desired, instead of their separate values. They are given by the following formula, a combination of 5-5 and 5-6.

$$\begin{aligned} f &= \frac{F}{A}+\frac{Fey}{I}\pm\frac{My}{I} \\ &= \frac{F}{A}\left(1\pm\frac{ey}{r^2}\right)\pm\frac{My}{I} \\ &= \frac{F}{A}\pm(Fe\pm M)\frac{y}{I} \end{aligned} \tag{5-7}$$

Any of these three forms may be used, whichever happens to be the most convenient. But, to be strictly correct, the section used in computing y and I must correspond to the actual section at the application of the force. It quite frequently happens that the prestress F acts on the net concrete section, while the external loads act on the transformed section. Judgment should be exercised in deciding whether refinement is necessary or whether approximation is permissible for each particular case.

When prestress eccentricity and external moments exist along two principal axes, the general elastic formula can be used.

$$\begin{aligned} f &= \frac{F}{A}\pm\frac{Fe_x x}{I_x}\pm\frac{Fe_y y}{I_y}\pm\frac{M_x x}{I_x}\pm\frac{M_y y}{I_y} \\ &= \frac{F}{A}\pm(Fe_x\pm M_x)\frac{x}{I_x}\pm(Fe_y\pm M_y)\frac{y}{I_y} \end{aligned} \tag{5-8}$$

EXAMPLE 5-4

A posttensioned bonded concrete beam, Fig. 5-8, has a prestress of 350 kips (1,557 kN) in the steel immediately after prestressing, which eventually reduces to 300 kips (1334 kN)

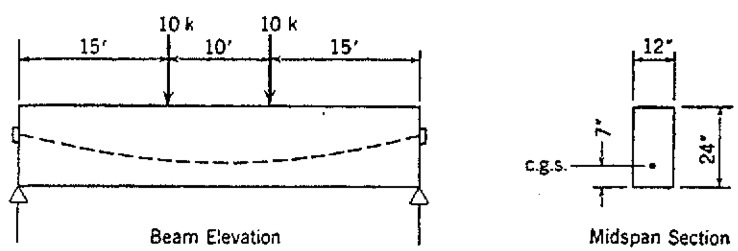

Fig. 5-8. Example 5-4.

due to losses. The beam carries two live loads of 10 kips (44.48 kN) each in addition to its own weight of 300 plf (4.377 kN/m). Compute the extreme fiber stresses at midspan, (*a*) under the initial condition with full prestress and no live load, and (*b*) under the final condition, after the losses have taken place, and with full live load.

Solution To be theoretically exact, the net concrete section should be used up to the time of grouting, after which the transformed section should be considered. This is not deemed necessary, and an approximate but sufficiently exact solution is given below, using the gross section of concrete at all times that is,

$$I = 12\times 24^3/12 = 13{,}800\text{ in.}^4\ (5744\times 10^6\text{ mm}^4)$$

1. *Initial condition*. Dead-load moment at midspan, assuming that the beam is simply supported after prestressing:

$$M=\frac{wL^2}{8}=\frac{300\times 40^2}{8}=60{,}000\text{ ft-lb }(81{,}360\text{ N}-\text{m})$$

$$f=\frac{F}{A}\pm\frac{Fey}{I}\pm\frac{My}{I}$$

$$=\frac{-350{,}000}{288}\pm\frac{350{,}000\times 5\times 12}{13{,}800}\pm\frac{60{,}000\times 12\times 12}{13{,}800}$$

$$=-1215+1520-625=-320\text{ psi }(-2.21\text{ N/mm}^2),\text{ top fiber}$$

$$=-1215-1520+625=-2110\text{ psi }(-14.55\text{ N/mm}^2),\text{ bottom fiber}$$

2. *Final condition*. Live-load moment at midspan = 150,000 ft-lb (203,400 N-m); therefore, total external moment = 210,000 ft-lb (284,760 N-m), while the prestress is reduced to 300,000 lb (1,334 kN); hence,

$$f=\frac{-300{,}000}{288}\pm\frac{300{,}000\times 5\times 12}{13{,}800}\pm\frac{210{,}000\times 12\times 12}{13{,}800}$$

$$=-1040+1300-2190=-1930\text{ psi }(-13.31\text{ N/mm}^2),\text{ top fiber}$$

$$=-1040-1300+2190=-150\text{ psi }(-1.03\text{ N/mm}^2),\text{ bottom fiber}$$

Example 5-4 describes the conventional method of stress analysis for prestressed concrete, but it will be recalled that in section 1-2 another method of approach is described in which the center of pressure C in the concrete is set at distance a from the center of prestress T in the steel such that

$$Ta = Ca = M \tag{5-9}$$

By this method, the stresses in concrete are not treated as being produced by prestress and external moments separately, but are determined by the magnitude and location of the center of pressure C, Fig. 5-9. Most beams do not carry axial load, therefore, C equals T and is located at a distance from T.

$$a = M/T$$

Since the value of T is the value of F in a prestressed beam it is quite accurately known. Thus the computation of a for a given moment M is simply a

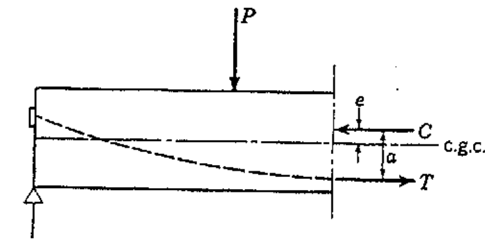

Fig. 5-9. Internal resisting couple C-T with arm a.

matter of statics. Once the center pressure C is located for a concrete section, the distribution of stresses can be determined either by the elastic theory or by the plastic theory. Generally the elastic theory is followed, in which case we have, since

$$C=T=F,\qquad f=\frac{C}{A}\pm\frac{Cey}{I}=\frac{F}{A}\pm\frac{Fey}{I} \tag{5-10}$$

where e is the eccentricity of C, not of F.

Following this approach, a prestressed beam is considered similar to a reinforced-concrete beam with the steel supplying the tensile force T, and the concrete supplying the compressive force C. C and T together form a couple resisting the external moment. Hence the value of A and I to be used in the above formula should be the net section of the concrete, and not the transformed section. If a beam has conduits grouted for bond, the stress in the grout is actually different from that in the adjacent concrete, and an exact theoretical solution would be quite involved. Under such conditions it is advisable to use the gross section of concrete for all computations for the sake of simplicity. Only when investigating the stresses before grouting should the net concrete section be used and even this refinement may not be required in most cases for design.

It can be noted that formula 5-10 is only a different form of formula 5-7, with e measured to C, thus combining the effect of M with the eccentricity of F. Although the formulas are in fact identical, the approaches are different. By following this second approach, all the inaccuracies are thrown into the estimation of the effective prestress in steel, which can generally be estimated within 5%. After that, the location of C is a simple problem in statics, and the distribution of C across the section can be easily computed or visualized. This method of approach will be further explained in the next chapter on the design of beam sections.

EXAMPLE 5-5

For the same problem as in example 5-4, compute the concrete stresses under the final loading conditions by locating the center of pressure C for the concrete section.

Solution Referring to Fig. 5-10, a is computed by

$$a=(210\times 12)/300=8.4\text{ in. }(213\text{ mm})$$

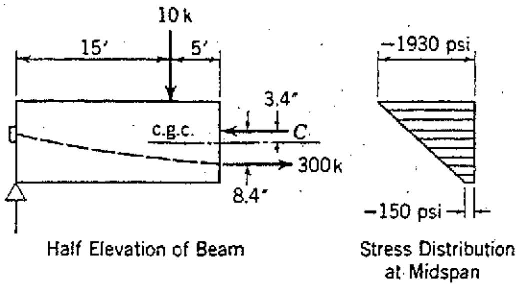

Fig. 5-10. Example 5-5.

Hence e for C is $8.4-5=3.4$ in. Since $C=F=300{,}000$ lb (1,334 kN).

$$f=\frac{C}{A}\pm\frac{Cey}{I}$$

$$=\frac{-300{,}000}{288}\pm\frac{300{,}000\times 3.4\times 12}{13{,}800}$$

$$=-1040-890=-1930 \text{ psi } (-13.31 \text{ N/mm}^2), \text{ top fiber}$$

$$=-1040+890=-150 \text{ psi } (-1.03 \text{ N/mm}^2), \text{ bottom fiber}$$

Also, by inspection, since the center of pressure is near the third point, the stress distribution should be nearly triangular as is shown. By comparing this solution with that for example 5-4, the directness and simplicity of this method seem to be evident.

5-4 Stresses in Steel Due to Loads

In prestressed concrete, prestress in the steel is measured during tensioning operations, then the losses are computed or estimated as described in Chapter 4. When dead and live loads are applied to the member, minor changes in stress will be induced in the steel. In a reinforced-concrete beam, steel stresses are assumed to be directly proportional to the external bending moment. When there is no moment, there is no stress. When the moment increases, the steel stresses increase in direct proportion. This is not true for a prestressed-concrete beam, whose resistance to external moment is furnished by a lengthening of the lever arm between the resisting forces C and T which remain relatively unchanged in magnitude.

In order to get a clear understanding of the behavior of a prestressed-concrete beam, it will be interesting to first study the variation of steel stress as the load increases. For the midspan section of a simple beam, the variation of steel stress with load on the beam is shown in Fig. 5-11. Along the X-axis is plotted the load on the beam, and along the Y-axis is plotted the stress in the steel. As prestress is applied to the steel, the stress in the steel changes from A to B, where B is at the

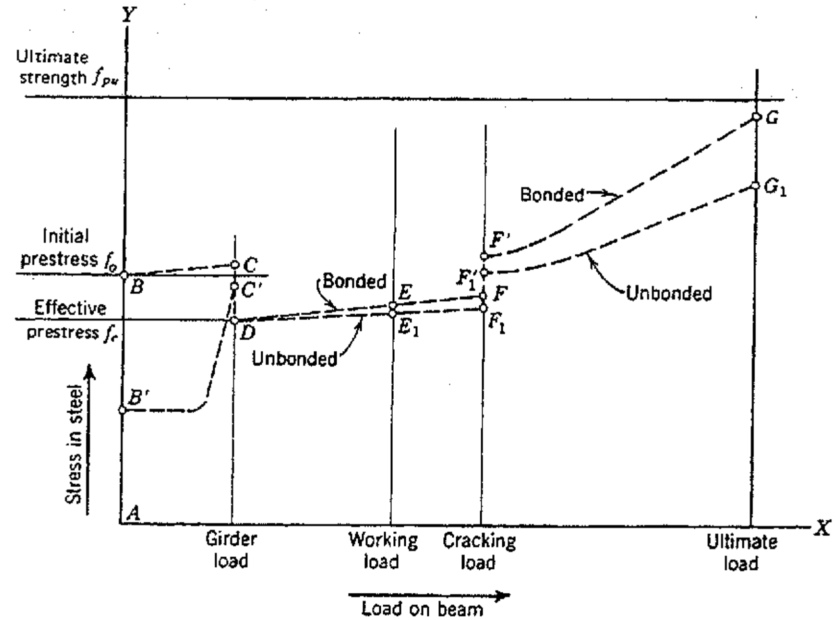

Fig. 5-11. Variation of steel stress with load.

level of f_0, which is the initial prestress in the steel after losses due to anchorage and elastic shortening have taken place.

Immediately after transfer, no load will yet be carried by the beam if it is supported on its falsework and if it is not cambered upward by the prestress. As the falsework is removed, the beam carries its own weight and deflects downward slightly, thus changing the stress in the steel, increasing it from B to C. When the dead weight of the beam is relatively light, then it can be bowed upward during the course of the transfer of prestress. The beam may actually begin to carry load when the average prestress in the steel is somewhere at B'. There may be a sudden breakaway of the beam's soffit from the falsework so that the weight of the beam is at once transferred to be carried by the beam itself, or the weight may be transferred gradually, depending on the actual conditions of support. But, in any event, the stress in steel will increase from B' up to point C'. The stress at C' is slightly lower than f_0 by virtue of the loss of prestress in the steel as caused by the upward bending of the beam. Consider now that the losses of prestress take place so that the stress in the steel drops from C or C' to some point D, representing the effective prestress f_e for the beam. Actually, the losses will not take place all at once but will continue for some length of time. However, for convenience in discussion, let us assume that all the losses take place before the application of superimposed dead and live loads.

Now let us add live load on the beam until the full-design working load is on it. The beam will bend and deflect downward, and stress in the steel will increase. For a bonded beam, such increase can be simply computed by the usual elastic theory,

$$\Delta f_s = n f_c = n \frac{My}{I}$$

where I and y correspond to the transformed section, and n is the modular ratio of steel to concrete. Since the maximum change in concrete stresses at the level of steel is not more than about 2000 psi (13.79 N/mm^2) in most cases, the corresponding change of stress in steel is limited to $2000n$, or 12,000 psi (82.74 N/mm^2) for a value of $n=6$. This stage is represented by the line DE in Fig. 5-11. It is significant to note that, in prestressed concrete, the variation in steel stress for working loads is limited to a range of about 12,000 psi (82.74 N/mm^2) even though the prestress is probably as high as 150,000 psi (1,034 N/mm^2).

If the beam is overloaded, beyond its working load and up to the point of cracking, the increase in steel stress still follows the same elastic theory. Hence the line DE is prolonged to point F. This would represent a tensile stress around 500 psi (3.45 N/mm^2) in the concrete at the level of steel indicating an increase in steel stress of about $6 \times 500 = 3000$ psi (20.68 N/mm^2) from E to F.

When the section cracks, there is a sudden increase of stress in the steel, from F to F' for the bonded beam. After cracking, the stress in the steel will increase faster with the load. As the load is further increased, the section will gradually approach its ultimate strength, the lever arm for the internal C-T couple cannot be increased any more, and increase in load is accompanied by a proportional increase in steel stress. This continues up to the point of failure. From the results of various tests, it is known that the stress in the steel approaches very nearly its ultimate strength at the rupture of the beam provided compression failure does not start in the concrete and failure of the beam is not produced by shear or bond. Hence the stress curve can be approximately drawn as from F' to G, usually slightly below f_{pu}, the steel ultimate strength.

The computation of steel stress beyond cracking and up to the ultimate load is a problem which can be rather accurately solved by analysis as shown later in this chapter. But it must be pointed out that between the two points, F' and G, there is one point when the steel ceases to be elastic, elastic in the sense that no appreciable permanent set is caused by the external load. This point is the limit to which a structure, such as a bridge or a building, could ever be subjected without permanent damage, but it will be higher than service load level. If it can be conveniently determined, it may be a more significant criterion for design than the cracking or ultimate load for some special situations.

If the beam is unbonded, the stress in the steel will be different from the bonded beam. Assuming that the same effective prestress is obtained before the

addition of any external load, we can discuss the stress in an unbonded tendon as follows: Starting from point D, when load is added to the beam, the beam bends while the steel slips with respect to the concrete. Owing to this slip, the usual method of a composite steel and concrete section no longer applies. Before cracking of the concrete, stress in the concrete due to any external moment M is given by

$$f = \frac{My}{I}$$

where I and y refer to those for the net concrete section. But it must be remembered that the stress in the steel changes as load is applied, Fig. 5-12. Hence the question becomes more complicated.

At the section of maximum moment, the stress in an unbonded tendon will increase more slowly than that in a bonded tendon. This is because any strain in an unbonded tendon will be distributed throughout its entire length. Hence, as the load is increased to the working or the cracking load, the steel stress will increase from D to E_1, F_1, and F_1', below E, F, and F', respectively, Fig. 5-11. To compute the average strain for the cable, it is necessary to determine the total lengthening of the tendon due to moments in the beam. This can be done by integrating the strain along the entire length. Let M be the moment at any point of an unbonded beam; the unit strain in concrete at any point is given by

$$\delta = \frac{f}{E} = \frac{My}{E_c I}$$

The total strain along the cable is then

$$\Delta = \int \delta \, dx = \int \frac{My}{E_c I} dx$$

The average strain is

$$\frac{\Delta}{L} = \int \frac{My}{L E_c I} dx$$

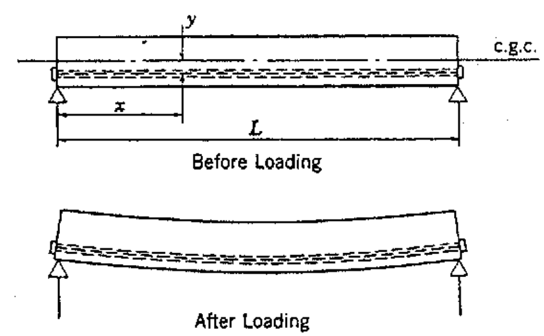

Fig. 5-12. Change of cable length in an unbonded beam.

The average stress is

$$f_s = E_s \frac{\Delta}{L} = \int \frac{M y E_s}{L E_c I} dx = \frac{n}{L} \int \frac{My}{I} dx \qquad (5\text{-}10)$$

If y and I are constant and M is an integrable form of x, the solution of this integral is simple. Otherwise, it will be easier to use a graphical or an approximate integration.

After cracks have developed in the unbonded beam, stress in the steel increases more rapidly with the load, but again it does not increase as fast as that at the maximum moment section in a similar bonded beam. In an unbonded beam, it is generally not possible to develop the ultimate strength of the steel at the rupture of the beam. Thus the stress curve is shown going up from F_1' to G_1, with G_1 below G by an appreciable amount. It is evident that the ultimate load for an unbonded beam is less than that for a corresponding bonded one, although there may be very little difference between the cracking loads for the two beams. There is a tendency for the unbonded beams to develop large cracks before rupture. These large cracks tend to concentrate strains at some localized sections in the concrete, thus lowering ultimate strength. Therefore, the strength of unbonded beams may be appreciably increased by the addition of nonprestressed bonded reinforcements, which tend to spread the cracks and to limit their size, as well as to contribute toward the tensile force in the ultimate resisting couple. The ACI Code specifies minimum amounts of such supplemental bonded reinforcement.

EXAMPLE 5-6

A posttensioned simple beam on a span of 40 ft is shown in Fig. 5-13. It carries a superimposed load of 750 plf in addition to its own weight of 300 plf. The initial prestress in the steel is 138,000 psi, reducing to 120,000 psi after deducting all losses and assuming no bending of the beam. The parabolic cable has an area of 2.5 sq in., $n = 6$. Compute the stress in the steel at midspan, assuming: (1) the steel is bonded by grouting: (2) the steel is unbonded and entirely free to slip. (Span = 12.2 m, superimposed load = 10.94 kN/m, self-weight = 4377 kN/m, initial prestress = 951.5 N/mm², effective prestress = 827.4 N/mm², and cable area = 1613 mm².)

Solution

1. Moment at midspan due to dead and live loads is

$$\frac{wL^2}{8} = \frac{(300+750)40^2}{8}$$
$$= +210{,}000 \text{ ft-lb } (+284{,}760 \text{ N-m})$$

Moment at midspan due to prestress is

$$2.5 \times 120{,}000 \times \tfrac{5}{12} = -125{,}000 \text{ ft-lb } (-169{,}500 \text{ N-m})$$

Net moment at midspan is 210,000 − 125,000 = 85,000 ft-lb (115,260 N − m). Stress in concrete at the level of steel due to bending, using I of gross concrete section, is

$$= \frac{My}{I} = \frac{85{,}000 \times 12 \times 5}{13{,}800} = 370 \text{ psi } (2.55 \text{ N/mm}^2)$$

Stress in steel is thus increased by

$$f_s = nf_c = 6 \times 370 = 2220 \text{ psi } (15.31 \text{ N/mm}^2)$$

Resultant stress in steel = 122,220 psi (842.7 N/mm²) at midspan.

Solution

2. If the cable is unbonded and free to slip, the average strain or stress must be obtained for the whole length of cable as given by formula 5-10,

$$f_s = \frac{n}{L} \int \frac{My}{I} dx$$

Using y_0 and M_0 for those at midspan and measuring x from the midspan, we can

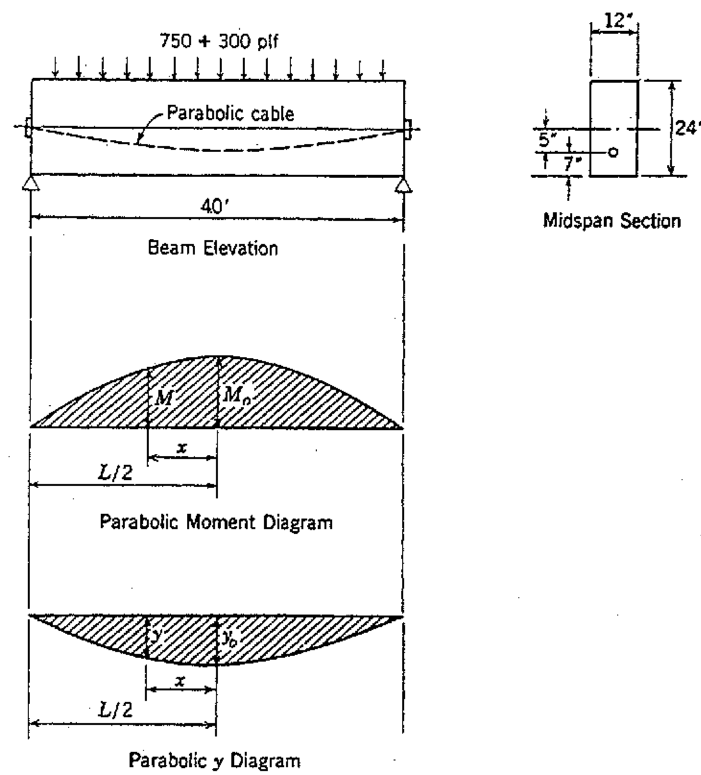

Fig. 5-13. Example 5-6.

express y and M in terms of x, thus,

$$M=M_0\left[1-\left(\frac{x}{L/2}\right)^2\right]$$

$$y=y_0\left[1-\left(\frac{x}{L/2}\right)^2\right]$$

$$f_s=\frac{n}{LI}\int_{-L/2}^{+L/2}M_0y_0\left[1-\left(\frac{x}{L/2}\right)^2\right]^2dx$$

$$=\frac{nM_0y_0}{LI}\left[x-\frac{2}{3}\frac{x^3}{(L/2)^2}+\frac{x^5}{5(L/2)^4}\right]_{-L/2}^{+L/2}$$

$$=\frac{8}{15}\left(\frac{nM_0y_0}{I}\right)$$

which is $\frac{8}{15}$ of the stress for midspan of the bonded beam, or $\frac{8}{15}(2220)=1180$ psi (8.14 N/mm^2).

Resultant stress in steel is $120{,}000+1180=121{,}180$ psi (835.5 N/mm^2) throughout the entire cable. In this calculation, the I of the gross concrete section is used and the effect of the increase in the steel stress on the concrete stresses is also neglected. But these are errors of the second order. Since the change in steel stress is relatively small, exact computations are seldom required in an actual design problem.

5-5 Cracking Moment

The moment producing first hair cracks in a prestressed concrete beam is computed by the elastic theory, assuming that cracking starts when the tensile stress in the extreme fiber of concrete reaches its modulus of rupture. Questions have been raised as to the correctness of this method. First, some engineers believed that concrete under prestress became a complex substance whose behavior could not be predicted by the elastic theory with any accuracy.[1] Then it was further questioned whether the usual bending test for modulus of rupture could give values to represent the tensile strength of concrete in a prestressed beam. However, most available test data seem to indicate that the elastic theory is sufficiently accurate up to the point of cracking, and the method is currently used. The ACI Code value for modulus of rupture, f_r, is $7.5\sqrt{f'_c}$ with units for both f_r and f'_c as psi.

Attention must be paid to the fact that the modulus of rupture is only a measure of the beginning of hair cracks which are often invisible to the naked eye. A tensile stress higher than the modulus is necessary to produce visible cracks. On the other hand, if the concrete has been previously cracked by overloading, shrinkage, or other causes, cracks may reappear at the slightest tensile stress. If the beam is made of concrete blocks, the cracking strength will depend on the tensile strength of the joining material.

Referring to formula 5-7, if f_r is the modulus of rupture, it is seen that, when

$$-\frac{F}{A}-\frac{Fec}{I}+\frac{Mc}{I}=f_r$$

cracks are supposed to start. Transposing terms, we have the value of cracking moment given by

$$M=Fe+\frac{FI}{Ac}+\frac{f_rI}{c} \tag{5-11}$$

where f_rI/c gives the resisting moment due to modulus of rupture of concrete, Fe the resisting moment due to the eccentricity of prestress, and FI/Ac that due to the direct compression of the prestress.

Formula 5-11 can be derived from another approach. When the center of pressure in the concrete is at the top kern point, there will be zero stress in the bottom fiber. The resisting moment is given by the prestress F times its lever arm measured to the top kern point, (see Appendix A for definition of kern points k_t and k_b), Fig. 5-14, thus,

$$M_1=F\left(e+\frac{r^2}{c}\right)$$

Additional moment resisted by the concrete up to its modulus of rupture is $M_2=f_rI/c$. Hence the total moment at cracking is given by

$$M=M_1+M_2=F\left(e+\frac{r^2}{c}\right)+\frac{f_rI}{c} \tag{5-12}$$

which can be seen to be identical with formula 5-11.

In order to be theoretically correct when applying the above two formulas, care must be exercised in choosing the proper section for the computation of I, r, e, and c. For computing the term f_rI/c, the transformed section should be used for bonded beams, while the net concrete section should be used for unbonded beams (proper modification being made for the value of prestress due

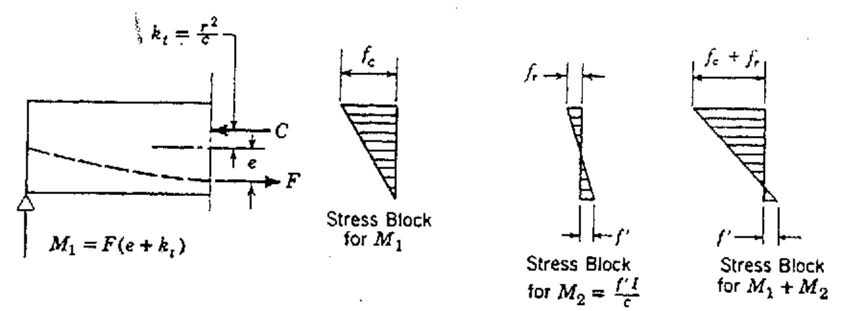

Fig. 5-14. Cracking moment.

to bending of the beam as explained in section 4-8). For the term $F\left(e+\frac{r^2}{c}\right)$, either the gross or the net section should be considered, depending on the computation of the effective prestress F. For a practical problem, these refinements are often unnecessary, and it will be easier to use one section for all the computations. In order to simplify the computations, the gross section of the concrete is most often used. If the area of holes is an important portion of the gross area, then net area may be used. If the percentage of steel is high, the transformed area may be preferred. The engineer must use discretion in choosing a method of solution consistent with the degree of accuracy required for his particular problem.

EXAMPLE 5-7

For the problem given in example 5-6, compute the total dead and live uniform load that can be carried by the beam, (1) for zero tensile stress in the bottom fibers, (2) for cracking in the bottom fibers at a modulus of rupture of 600 psi (4.14 N/mm^2), and assuming concrete to take tension up to that value.

Solution

1. Considering the critical midspan section and using the gross concrete section for all computations, k_t is readily computed to be at 4 in. (101.6 mm) above the middepth, Fig. 5-15. To obtain zero stress in the bottom fibers, the center of pressure must be located at the top kern point. Hence the resisting moment is given by the prestress multiplied by the lever arm, thus

$$F(e+k_t)=300(5+4)/12=225 \text{ k-ft } (305.1 \text{ kN-m})$$

Solution

2. Additional moment carried by the section up to beginning of cracks is

$$\frac{f_r I}{c}=\frac{600\times 13{,}800}{12}$$
$$=690{,}000 \text{ in.-lb}$$
$$=57.6 \text{ k-ft } (78.1 \text{ kN}-\text{m})$$

Total moment at cracking is $225+57.6=282.6$ k-ft (383.2 kN-m), which can also be obtained directly by applying formula 5-11 or 5-12.

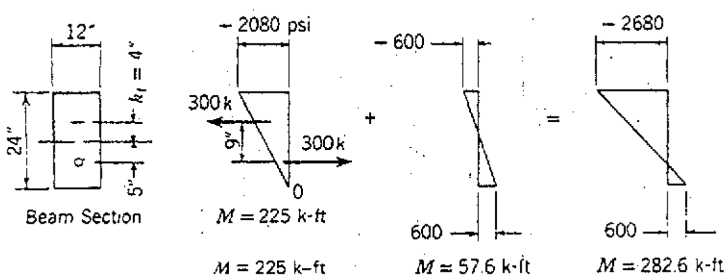

Fig. 5-15. Example 5-7.

5-6 Ultimate Moment—Bonded Tendons

Exact analysis for the ultimate strength of a prestressed-concrete section under flexure is a complicated theoretical problem, because both steel and concrete are generally stressed beyond their elastic range. The following section develops such an analysis technique for bonded beams. However, for the purpose of practical design, where an accuracy of 5-10% is considered sufficient, relatively simple procedures can be developed.

Many tests have been run, and many papers written, on the ultimate flexural strength of prestressed concrete sections. Worthy of special mention are the group of papers on this thesis[2] presented before the First International Congress on Prestressed Concrete held in London, October 1953, and another summary paper presented at the Third Congress of the International Federation for Prestressing.[3] In the United States, laboratory investigations carried out at the University of Illinois and the Portland Cement Association gave the results of extensive tests, together with definite recommendations.[4,5,6] Although formulas for ultimate strength proposed by various authors seem to differ greatly on the surface, they generally yield values within a few per cent of one another. Hence it can be concluded that the ultimate strength of prestressed concrete under flexure can be predicted with sufficient accuracy.

A simple method for determining ultimate flexural strength following the ACI Code is presented herewith, based on the results of the aforementioned tests as well as others. This method is limited to the following conditions.

1. The failure is primarily a flexural failure, without shear, bond, or anchorage failure which might decrease the strength of the section.
2. The beams are bonded. Unbonded beams possess different ultimate strength and are discussed later.
3. The beams are statically determinate. Although the discussions apply equally well to individual sections of continuous beams, the ultimate strength of continuous beams as a whole is explained by the plastic hinge theory to be discussed in Chapter 10.
4. The load considered is the ultimate load obtained as the result of a short static test. Impact, fatigue, or long-time loadings are not considered.

Of the methods proposed for determining the ultimate flexural strength of prestressed-concrete sections, some are purely empirical and others highly theoretical. The empirical methods are generally simple but are limited only to the conditions which were encountered in the tests. The theoretical ones are intended for research studies and hence unnecessarily complicated for the designer. For the purpose of design, a rational approach is presented in the following, consistent with test results, but neglecting refinements so that reasonably correct values can be obtained with the minimum amount of effort. The method is based on the simple principle of a resisting couple in a prestressed beam, as that in any other beam. At the ultimate load, the couple is made of two forces, T' and C', acting with a lever arm a'. The steel supplies the tensile force T', and the concrete, the compressive force C'.

Before going any further with the method, let us first study the modes of failure of prestressed-beam sections. The failure of a section may start either in the steel or in the concrete, and may end up in one or the other. The most general case is that of an underreinforced section, where the failure starts with the excessive elongation of steel and ends with the crushing of concrete. This type of failure occurs in both prestressed- and reinforced-concrete beams, when they are underreinforced. Only in some rare instances may fracture of steel occur in such beams; that happens, for example, when the compressive flange is restrained and possesses a higher actual strength. A relatively uncommon mode of failure is that of an overreinforced section, where the concrete is crushed before the steel is stressed into the plastic range. Hence there is only a limited amount of deflection before rupture, and a brittle mode of failure is obtained. This is similar to an overreinforced nonprestressed-concrete beam. Another unusual mode of failure is that of a too lightly reinforced section, where failure may occur by the breaking of the steel immediately following the cracking of concrete. This happens when the tensile force in the concrete is suddenly transferred to the steel whose area is too small to absorb that additional tension.

There is no sharp line of demarcation between the percentage of reinforcement for an overreinforced beam and that for an underreinforced one. The transition from one type to another takes place gradually as the percentage of steel is varied. A sharp definition of "balanced condition" cannot be made since the steel used for prestressing does not exhibit a sharp yield point. For the materials presently used in prestressed work, the reinforcement index, ω_p, which approximates the limiting value to assure that the prestressed steel (A_{ps}) will be slightly into its yield range, is given by the ACI Code as follows:

$$\omega_p = \rho_p f_{ps}/f'_c \leqslant 0.30 \qquad (5\text{-}13)$$

where

$$\rho_p = A_{ps}/bd$$

There are situations where prestressing steel (A_{ps}) and ordinary reinforcing bars (A_s) are used together in a prestressed beam. In this case the total of all the tension steel is considered along with the possibility of compression steel (A'_s). The limiting reinforcement ratio is given as

$$(\omega + \omega_p - \omega') \leqslant 0.30 \qquad (5\text{-}14)$$

where

$$\omega = \rho f_y/f'_c \quad \text{and} \quad \rho = A_s/bd$$
$$\omega' = \rho' f_y/f'_c \quad \text{and} \quad \rho' = A'_s/bd$$

Such ratios of reinforcement almost always end in plastic failure and can be termed as underreinforced ratios. If the ratio from equation 5-14 is over 1.0, sudden crushing of concrete without substantial elongation of steel will be likely to take place. If it is less than about 0.10, breaking of the wires following cracking of concrete may occur.

A proper definition of the percentage of steel ρ is important for prestressed sections because of their irregular shapes. For ultimate strength it is not the total concrete area or the shape of cross section but the concrete area in the compressive flange that matters; hence ρ will be more indicative of the relative strength of concrete and steel if it is expressed in terms of A_s/bd, where b is the width or average width of the compressive flange and d the effective depth as indicated above for the ACI Code expressions.

ACI Code Bonded Beams. For underreinforced bonded beams following the ACI Code, the steel is stressed to a stress level which approaches its ultimate strength at the point of failure for the beam in flexure. For the purpose of practical design, it will be sufficiently accurate to assume that the steel is stressed to the stress level, f_{ps}, given by the equation for bonded beams from the ACI Code which closely approximates test results.[6] Provided the effective prestress, f_{se}, is not less than $0.5 f_{pu}$, the following approximate value for the steel stress at ultimate moment capacity for the beam is applicable for bonded beams:

$$f_{ps} = f_{pu}\left(1 - 0.5\rho_p \frac{f_{pu}}{f'_c}\right) \qquad (5\text{-}15)$$

Note that as the steel ratio ρ_p is reduced, the member is increasingly underreinforced; and the steel stress f_{ps} approaches the ultimate strength of prestressing steel. In fact, there are some test data which seem to show that the steel was stressed even beyond its ultimate strength. Though this does not seem to be possible, it might perhaps be explained by the fact that the group strength of wires forced to fail together at one section of a beam might be higher than the tested strength of steel in the specimens, since, during specimen tests, only the strength of the weakest link is recorded.

The computation of the ultimate resisting moment is a relatively simple matter and can be carried out as follows. Referring to Fig. 5-16, the ultimate compressive force in the concrete C' equals the ultimate tensile force in the steel T', thus,

$$C' = T' = A_s f_{ps}$$

Let a' be the lever arm between the forces C' and T'; then the ultimate resisting moment is given by

$$M' = T'a' = A_s f_{ps} = M_n \text{ (ACI Code nominal strength)}$$

To determine the lever arm a', it is only necessary to locate the center of pressure C'. There are many plastic theories for the distribution of compressive

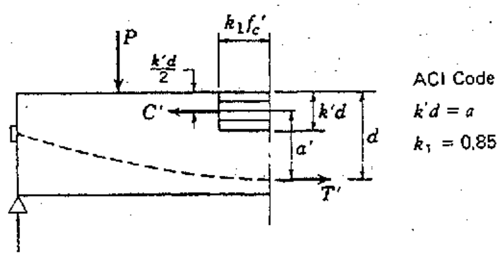

Fig. 5-16. Ultimate moment.

stress in concrete at failure,[7] assuming the stress block to take the shape of a rectangle, trapezoid, parabola, etc. Although the actual stress distribution is a very interesting problem for research, for the purpose of design, any of these methods would be sufficiently accurate, because they would yield nearly the same lever arm a', seldom differing by more than 5%.

Choosing the simplest stress block, a rectangle, for the ultimate compression in concrete, the depth to the ultimate neutral axis $k'd$ is computed by

$$C' = k_1 f_c' k'bd$$

where $k_1 f_c'$, is the average compressive stress in concrete at rupture. Hence,

$$k'd = \frac{C'}{k_1 f_c' b} = \frac{A_{ps} f_{ps}}{k_1 f_c' b}$$

$$k' = \frac{A_s f_{ps}}{k_1 f_c' bd} \tag{5-16}$$

These formulas apply if the compressive flange has a uniform width b at failure.

Locating C' at the center of the rectangular stress block, we have the lever arm

$$a' = d - k'd/2$$

$$= d\left(1 - \frac{k'}{2}\right) \tag{5-17}$$

Hence, the ultimate resisting moment is

$$M' = A_{ps} f_{ps} d\left(1 - \frac{k'}{2}\right) = M_n \text{ (ACI notation)} \tag{5-18}$$

Now the determination of the value of k_1 deserves some comments. According to Whitney's plastic theory of reinforced-concrete beams, k_1 should be 0.85, based on cylinder strength. According to some authors in Europe, k_1 should be 0.60 to 0.70 based on the cube strength; since cube strength is 25% higher than cylinder strength, this would give approximately 0.75 to 0.88 for k_1 based on the cylinder strength. The important thing for the designer to see is the fact that

variation of the value of k_1 does not appreciably affect the lever arm a'. Hence it is considered accurate enough to adopt some approximate value, such as 0.85 for k_1. Using 0.85 for k_1, formula 5-16 can be written as

$$k' = \frac{A_{ps} f_{ps}}{0.85 f_c' bd} \tag{5-19}$$

By substituting this expression for k' into equation 5-18, we have

$$M' = A_{ps} f_{ps} d\left(1 - \frac{A_{ps} f_{ps}}{2 \times 0.85 f_c' bd}\right) \tag{5-20}$$

For a rectangular section for the compression area, we can let $\rho_p = A_{ps}/bd$. Then we have the following formula:

$$M' = A_{ps} f_{ps} d\left(1 - \frac{0.59 \rho_p f_{ps}}{f_c'}\right) \tag{5-21}$$

or from Fig. 5-16 with ACI notation $k'd = a$

$$M_n = A_{ps} f_{ps}\left(d - \frac{a}{2}\right) \tag{5-22}$$

which is identical to that given in the commentary of the American Concrete Institute and as first proposed by the ACI-ASCE Recommendations.[8]

The ACI Code introduces the strength reduction factor, ϕ, and writes equation 5-21 in terms of ω_p to solve the design ultimate moment as follows:

$$M_u = \phi\left[A_{ps} f_{ps} d(1 - 0.59\omega_p)\right] \tag{5-23}$$

The alternative equation (5-22) written directly in terms of the T' and C' force couple becomes the following ACI Code design ultimate moment equation:

$$M_u = \phi\left[A_{ps} f_{ps}\left(d - \frac{a}{2}\right)\right] \tag{5-24}$$

For flexure the ACI Code uses $\phi = 0.9$ in the two equations for M_u given above, (5-23) and (5-24). These expressions apply to rectangular beams or beams which have a rectangular-shaped compression zone for the concrete cross section.

EXAMPLE 5-8

An I-shaped beam is prestressed with $A_{ps} = 2.75$ in.^{2} as prestressing steel with an effective stress, f_{se}, of 160 ksi. The c.g.s. of the strands which supply the prestress is 4.5 in. above the bottom of the beam as shown in Fig. 5-17 along with the shape of the concrete cross section. Material properties are: $f_{pu} = 270$ ksi; $f_c' = 7000$ psi. Find the ultimate resisting moment for the section for design following the ACI Code. ($A_{ps} = 1{,}774$ mm^2, $f_{se} = 1{,}103$ N/mm^2, $f_{pu} = 1{,}862$ N/mm^2, and $f_c' = 48$ N/mm^2.)

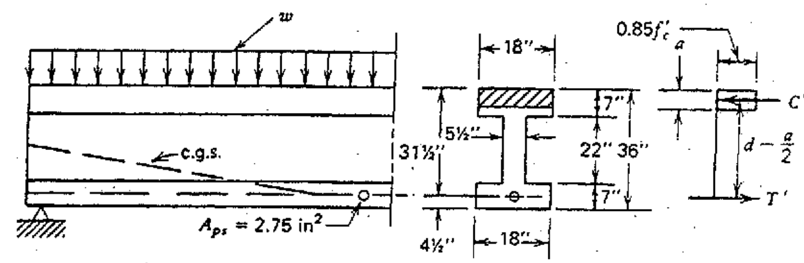

Fig. 5-17. Example 5-8.

Solution:

$$\rho_p=\frac{2.75}{(18)(31.5)}=0.00485$$

Estimate steel stress at ultimate by the ACI equation (5-15) which is valid to use since $f_{se}=160$ ksi (1103 N/mm^2) $>0.5f_{pu}=135$ ksi (931 N/mm^2).

$$f_{ps}=270{,}000\left[1-(0.5)(0.00485)\left(\frac{270{,}000}{7{,}000}\right)\right] \qquad (5\text{-}15)$$

$$f_{ps}=245{,}000 \text{ psi}=245 \text{ ksi } (1689 \text{ N/mm}^2)$$

Check the reinforcement index

$$\omega_p=\frac{(0.00485)(245{,}000)}{7000}=0.17<0.30 \qquad (5\text{-}13)$$

Referring to Fig. 5-17 sketch of section

$$T'=A_{ps}f_{ps}=2.75\times 245=674 \text{ k } (2{,}998 \text{ kN})$$

$$C'=0.85f_c'\times 18\times a=674 \text{ k } (2{,}998 \text{ kN})$$

$$a=\frac{674}{(0.85)(7)(18)}=6.29 \text{ in.}<7 \text{ in. } O.K. \text{ rectangular section behavior}$$

$$M_n=T'\left(d-\frac{a}{2}\right)=674\left(31.5-\frac{6.29}{2}\right)=19{,}100 \text{ in.-k. } (2{,}158 \text{ kN-m}) \qquad (5\text{-}22)$$

$$M_u=0.9M_n=17{,}200 \text{ in.-k. } (1944 \text{ kN-m}) \qquad (5\text{-}24)$$

Note that even though the section in example 5-8 is I-shaped it behaves as a "rectangular section"; the compression zone of the concrete is rectangular as shown by the shaded area in Fig. 5-17. The following example illustrates the case where the compression zone is nonrectangular.

For flanged sections (nonrectangular compression zone) we may still use equation 5-15 to estimate the steel stress at ultimate, f_{ps}. The total area of prestressed steel, A_{ps}, is divided into two parts with A_{pf} developing the flanges and A_{pw} developing the web as shown in Fig. 5-18. The ultimate moment is simply computed from the two parts: the flange part has the compression resultant force acting at middepth of flange, $h_f/2$, and the arm of the moment

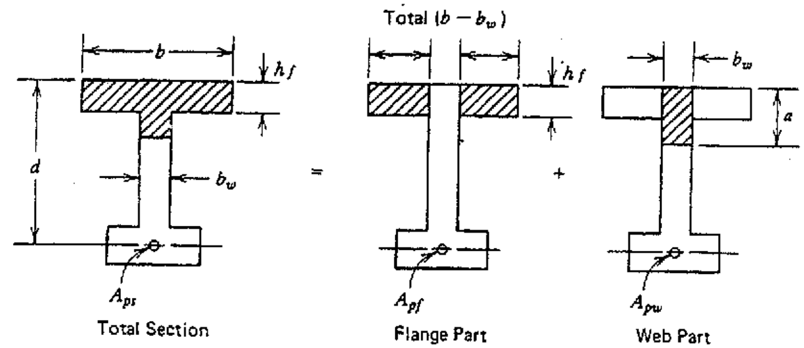

Fig. 5-18. Flanged section

couple is $\left(d-\frac{h_f}{2}\right)$; the web part has the compression resultant force acting at $a/2$ from the top the beam, and the arm of the moment couple is $\left(d-\frac{a}{2}\right)$. The equivalent rectangular stress block is assumed as before, Fig. 5-17, and the depth a is determined by the compression area required based on equal total compression and tension forces at ultimate. The commentary of the ACI Code contains equations for M_u to cover this case which it terms "flanged section."

$$M_u=\phi\left[A_{pw}f_{ps}\left(d-\frac{a}{2}\right)+0.85f_c'(b-b_w)h_f\left(d-\frac{h_f}{2}\right)\right. \qquad (5\text{-}25)$$

where

$$A_{pw}=A_{ps}-A_{pf} \qquad (5\text{-}26)$$

and

$$A_{pf}=0.85f_c'(b-b_w)h_f/f_{ps} \qquad (5\text{-}27)$$

EXAMPLE 5-9

The same I-shaped prestressed concrete beam as example 5-8 but the steel area is increased to $A_{ps}=3.67$ in.^{2} The effective steel stress remains 160 ksi. The c.g.s. of the strands is 4.5 in. above the bottom of the beam as shown in Fig. 5-19 along with the

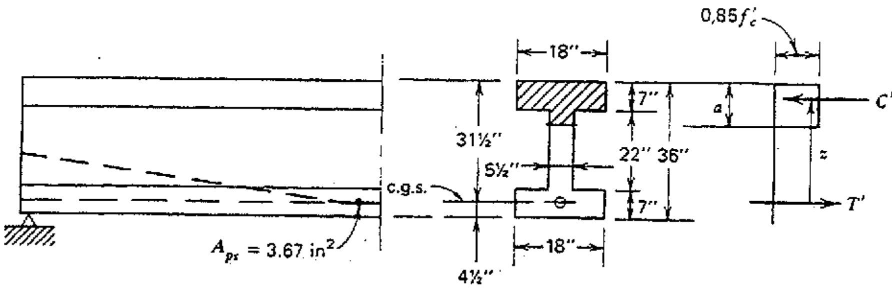

Fig. 5-19. Example 5-9.

shape of the cross section: material properties are same as example 5-8: $f_{pu}=270$ ksi, $f_c'=7000$ psi. Find the ultimate resisting moment for the section for design following the ACI Code. ($A_{ps}=2368$ mm^2, $f_{se}=1103$ N/mm^2, $f_{pu}=1862$ N/mm^2, and $f_c'=48$ N/mm^2)

Solution

$$\rho_p=\frac{3.67}{(18)(31.5)}=0.00647$$

Use equation 5-15 to estimate steel stress at ultimate.

$$f_{ps}=270{,}000\left[1-(0.5)(0.00647)\left(\frac{270{,}000}{7{,}000}\right)\right]$$

$$f_{ps}=236{,}000 \text{ psi}=236 \text{ ksi } (1627 \text{ N/mm}^2)$$

Check the reinforcement index after the flanged section is evaluated below.

Referring to Fig. 5-18 and 5-19 determine the extent of the compression zone

$$T'(\text{total})=(3.67)(236)=866 \text{ k } (3{,}852 \text{ kN})$$

$$\text{Area of compression zone}=\frac{866}{0.85f_c'}=145.5 \text{ in.}^2\ (93.87\times10^3 \text{ mm}^2)$$

$$\text{Flange area}=18\times7 \qquad =126.0 \text{ in.}^2\ (81.29\times10^3 \text{ mm}^2)$$

$$\text{Web area below flange} \qquad =19.5 \text{ in.}^2\ (12.58\times10^3 \text{ mm}^2)$$

$$a=7+\frac{19.5}{5.5}=7+3.55=10.55 \text{ in. } (268 \text{ mm})$$

This verifies that the section is behaving as "flanged" as shown by Fig. 5-18 and M_u can now be evaluated.

Referring to Fig. 5-18 and using ACI Commentary equations

$$A_{pf}=(0.85)(7000)(18.0-5.5)(7)/236{,}000=2.21 \text{ in.}^2\ (1426 \text{ mm}^2) \qquad (5\text{-}27)$$

$$A_{pw}=3.67-2.21=1.46 \text{ in.}^2\ (942 \text{ mm}^2) \qquad (5\text{-}26)$$

Check reinforcement index for the flanged section;

$$\rho_{pw}=A_{pw}/b_w d=1.46/(5.5)(31.5)=0.00843$$

$$\omega_{pw}=(0.00843)(236{,}000)/7000=0.284<0.30$$

$$M' \text{ for web part}=A_{pw}f_{ps}\left(d-\frac{a}{2}\right)$$

$$M'_{\text{web}}=(1.46)(236)\left(31.5-\frac{10.55}{2}\right)=9{,}040 \text{ in.-k } (1{,}021.5 \text{ kN}-\text{m})$$

$$M' \text{ for flange part}=0.85f_c'(b-b_w)h_f\left(d-\frac{h_f}{2}\right)$$

$$M'_{\text{flange}}=(0.85)(7.0)(18.0-5.5)(7)(31.5-7/2)=14{,}580 \text{ in.-k } (1647.5 \text{ kN}-\text{m})$$

$$M'_{\text{total}}=9040+14{,}580=23{,}620 \text{ in.-k } (2669 \text{ kN}-\text{m})=M_n$$

Note that the ACI commentary equation (5-25) contains these two terms, and

we may write it in the form:

$$M_u=\phi\left[M'_{\text{web}}+M'_{\text{flange}}\right]=\phi\left[M'_{\text{total}}\right]$$

thus

$$M_u=(0.9)(23{,}620)=21{,}260 \text{ in.-k } (2{,}402 \text{ kN}-\text{m})$$

The examples 5-8 and 5-9 illustrate the simplicity of analysis for M_u whether the section behaves as a "rectangular" or "flanged" section. It should be noted that the addition of more prestressed steel to the section in example 5-9 causes the section to almost reach the limit of reinforcement index, $\omega=0.30$, which the ACI Code would allow. Further addition of tension steel would cause the beam to be overreinforced, and the beam would not have a ductile failure. Addition of compression steel might be required to be sure that ductility is assured (equation 5-14). For the flanged section we use the web of the section with b_w and the steel area required to develop the compressive strength of the web only to find $\omega_{pw}\leqslant0.30$ as illustrated in example 5-9. The ACI Code has this requirement stated as follows: (similar to equation 5-14):

$$(\omega_w+\omega_{pw}-\omega_w')\leqslant0.30 \qquad (5\text{-}28)$$

The terms involving ordinary reinforcement are ω_w (tension steel) and ω_w' (compression steel) for equation 5-28. In equation 5-14 the corresponding terms are ω and ω'. Thus in prestressed concrete as in reinforced concrete analysis, addition of compression steel will add ductility as the steel (unstressed bars) on the compression side of the beam carries a part of the total compressive force, relieving compression that would otherwise be carried by the concrete.

Note also in example 5-9 that addition of more prestressing strand causes the steel stress at ultimate to be reduced. The stress-strain curve for the prestressing steel, Fig. 2-7, has the characteristic of continuing slight increase in stress with strain in excess of yield. The more ductile beam of example 5-8 ($\omega_p=0.17<0.30$) will fail in flexure with higher steel strain and $f_{ps}=245$ ksi; with added A_{ps} in example 5-9 ($\omega_{pw}=0.28<0.30$) we have less ductility, smaller steel strain at ultimate, and $f_{ps}=236$ ksi. This will be discussed later in connection with the more exact moment-curvature analysis, but the trends in behavior are important to observe in the ACI Code analysis, which gives results in good agreement with tests.

If material strengths and physical dimensions are in agreement with assumed values, the ultimate moment will be quite close to M' computed by the ACI Code analysis. The $\phi=0.9$ strength reduction factor adds safety in design, the intent being to allow for possible understrength in materials, dimensional errors in construction and errors in the assumptions made in analysis.

5-7 Moment-Curvature Analysis—Bonded Beams

A rational analysis which follows the behavior of a bonded prestressed concrete through the total load range from initial loading to failure has been developed,[6,9] and tests have shown the results of the analysis to be quite reliable. This moment-curvature analysis is derived from basic assumptions about materials and member behavior. The technique is described below, and a numerical example will show that the ultimate strength found by this more exact procedure is close to the ACI Code estimate, M'. But the added understanding of behavior which can be gained for the progressive load stages leading to failure is important to emphasize. This complete analysis is quite general, and computer programs have been written which perform the detailed calculations very rapidly. Hand calculation can be used as will be illustrated by the example problem.

The following assumptions are made in connection with the moment-curvature analysis:

1. Tendons are bonded to the concrete. *Changes* in strain in the steel and concrete after bonding are assumed to be the same.
2. The initial strain from the effective prestress in the tendon when no moment from applied loads acts on the section is illustrated by Fig. 5-20(*a*). At the level of steel, the concrete *compressive* strain, ϵ_{ce}, exists while the tendon has a *tensile* strain, ϵ_{se}, which corresponds to the stress f_{se}, which is initially effective.
3. Stress-strain properties for the materials are known or assumed (Fig. 5-21) for use in analysis.
4. Strains are assumed to be distributed linearly over the depth of the beam as shown in Fig. 5-20.
5. Tension and compression forces acting on the cross section must be in equilibrium for the beam which has only flexure without any applied axial load.

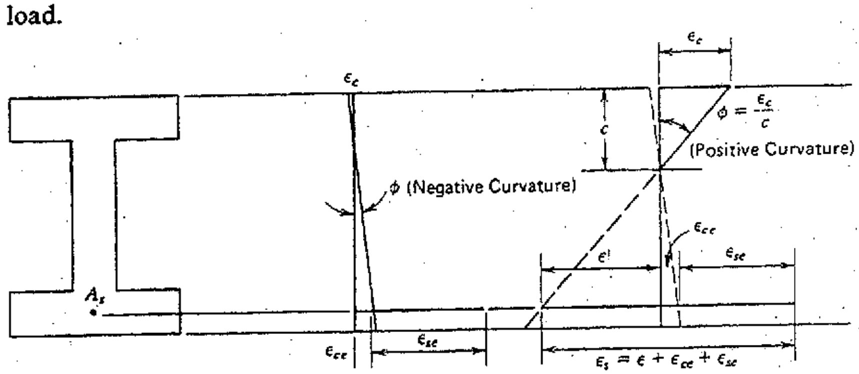

(*a*) Strain Distribution At Zero Moment (*b*) Strain Distribution After Moment Is Applied

Fig. 5-20. Distribution of strain assumed.

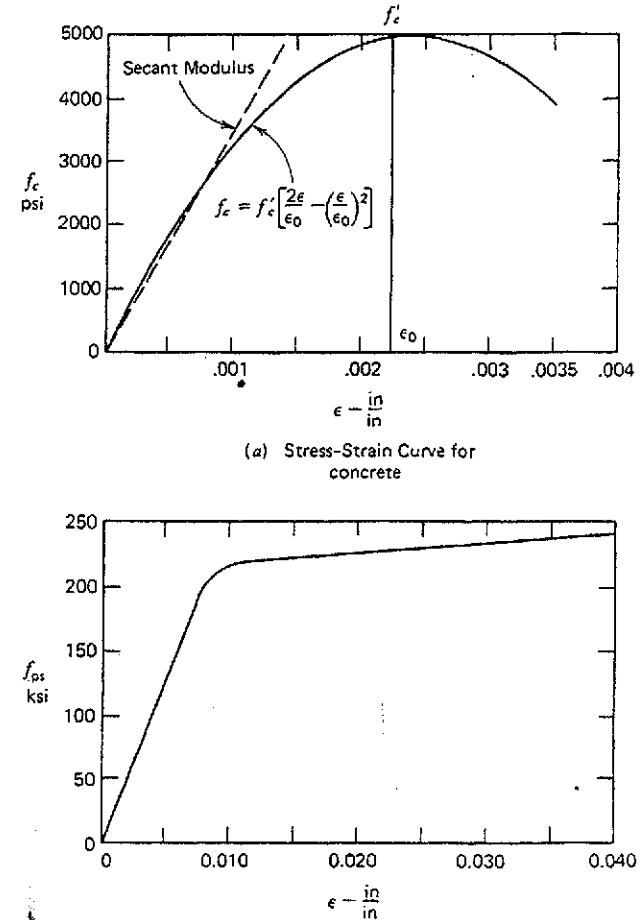

(*a*) Stress-Strain Curve for concrete

(*b*) Stress-Strain Curve for Steel

Fig. 5-21. Stress-strain properties for materials.

$$\text{Concrete stress} = f_c = f'_c\left[\frac{2\phi x}{\epsilon_0} - \left(\frac{\phi x}{\epsilon_0}\right)^2\right] \quad \text{as shown in Fig. 5-21c}$$

where $\phi x = \epsilon$ in the expression from Hognestad similar to Fig. 5-21a.

$$C_c = \int_0^c f_c b\, dx = bf'_c \int_0^c \left(\frac{2\phi x}{\epsilon_0} - \frac{\phi^2 x^2}{\epsilon_0^2}\right) dx \quad \text{(see Fig. 5-21c)}$$

solving this, the resultant compression force for a rectangular section is

$$C_c = bf'_c \frac{\phi}{\epsilon_0} c^2 \left[1 - \frac{\phi c}{3\epsilon_0}\right] \tag{5-29}$$

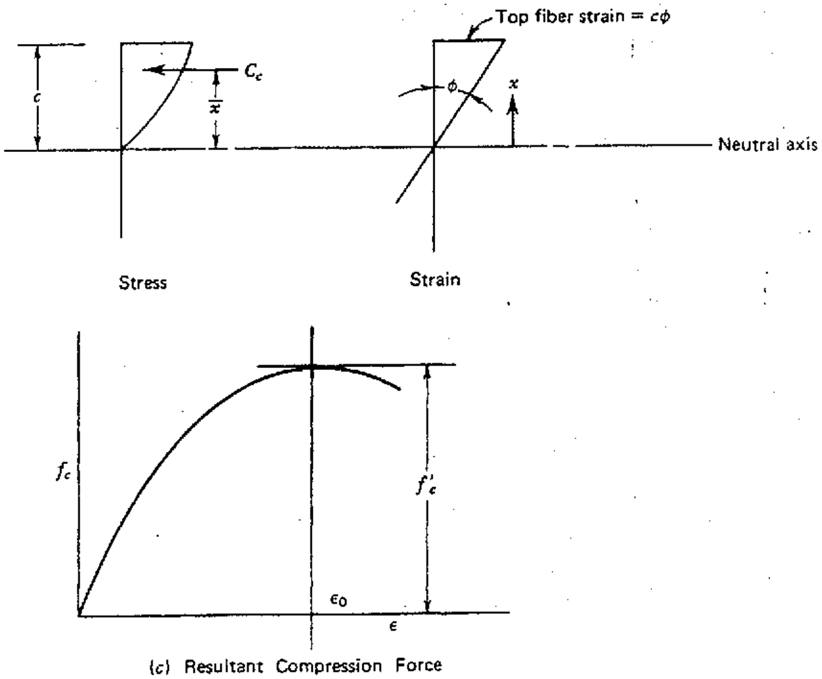

Fig. 5-21(c). Resultant Compression Force.

$\bar{x}C_c = \int_0^c (f_c b\, dx)x$ substituting the expression above for C_c and rearranging terms, the distance from neutral axis to line of action for resultant compression force is

$$\bar{x} = c\left[\frac{8\epsilon_0 - 3\phi c}{12\epsilon_0 - 4\phi c}\right] \tag{5-30}$$

6. Ultimate moment corresponds to the occurrence of a strain in the concrete which causes crushing (usually 0.003 in./in.) or a steel strain which would fracture the tendon (for most prestressing steel about 5% strain).
7. The failure analyzed is in flexure, and it is assumed that the member will have adequate shear strength to prevent failure. Bond and anchorage of steel is assumed adequate to prevent failure prior to reaching flexural strength at the section being analyzed.

The assumptions listed above are justified by experimental data, and a few comments are in order before describing the analysis procedure. Item 1 is extremely important; bonded pretensioned beams and posttensioned beams (grouted tendons following stressing) satisfy this assumption. Unbonded tendons will slip with respect to the concrete and thus will not satisfy this assumption of strain change compatibility for steel and concrete. Item 2 relates to the initial

strains which exist prior to the application of external moment. The steel will have experienced losses which would be estimated to find the effective stress, f_{se}, which exists as the starting point for analysis.

This leads to Item 3, the known stress-strain relationship for the steel, since the ϵ_{se} is simply the steel strain corresponding to f_{se} from this curve. The tests of typical materials used for tendons provide these data (Appendix B). The concrete stress-strain curve is assumed here as a parabolic form following Hognestad very closely. This is convenient because it allows integration to solve the resultant compressive force, and its location in a closed form solution as shown in Fig. 5-21(*c*). The secant modulus of elasticity for concrete, Fig. 5-21(*a*), is made to correspond to the ACI Code value for E_c, and E_s is taken from the stress-strain curve for the steel used in the beam. The initial response for the member prior to cracking (at tension in the concrete, $f_r = 7.5\sqrt{f'_c}$) is elastic, and the values of E_c and E_s relate stress to strain in the materials. As shown in Fig. 5-22 the value of f_r follows the ACI equation with scatter above or below this value.

Item 4 relates to linear strains over the depth of the member, which has been verified by tests of bonded beams where measurements were made over a gage length including cracks. Good bond of the steel results in the formation of numerous cracks as observed in tests of both pretensioned and posttensioned beams, and the average curvature is adequate to represent the beam response to moment, Fig. 5-23. This analysis deals with average curvatures with higher

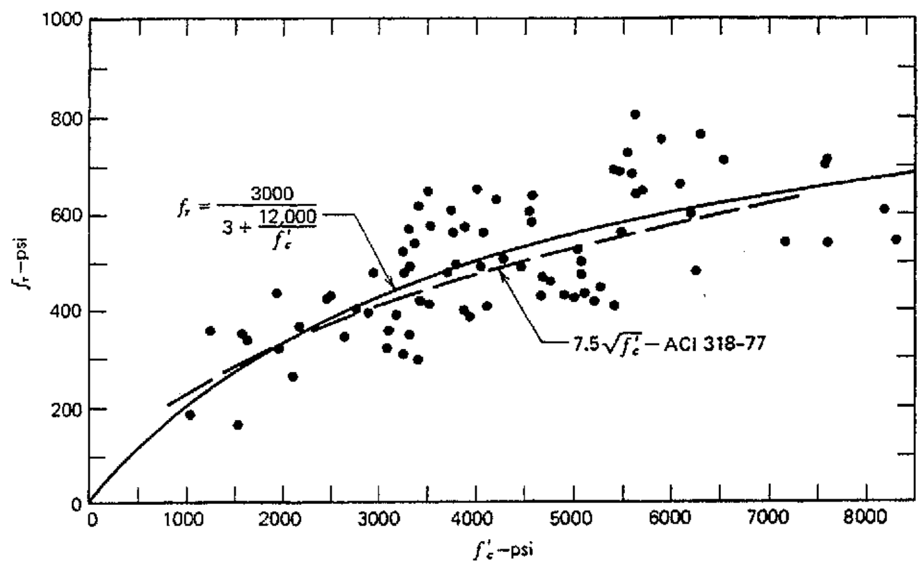

Fig. 5-22. Relationship between modulus of rupture and compressive strength of concrete.[10]

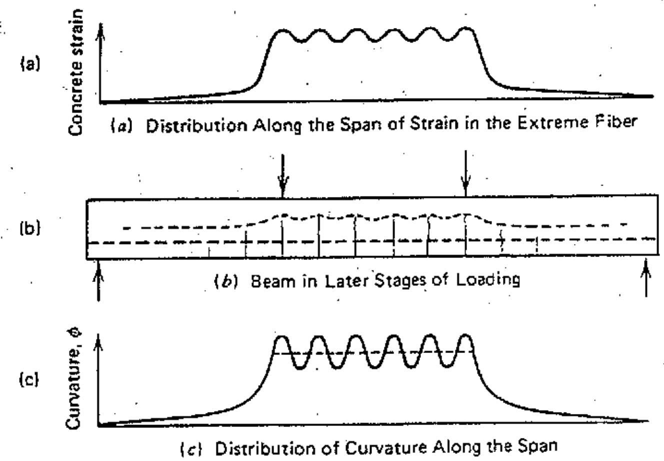

Fig. 5-23. Distribution of strain and curvature along the span.

values at a crack being averaged with lower values between cracks. The angle, ϕ, measured from the linear strains over the depth of the section is the curvature, Fig. 5-20. Note that this is initially negative as shown in Fig. 20(a), (camber results) but becomes positive curvature (downward deflection) as moment is added, Fig. 5-20(b).

The equilibrium of forces is implied from statics, but it is a key assumption here as Item 5. The total tension, T', acts together with an equal resultant compression, C'. The stress-strain curve for concrete together with the shape of the compression zone determine the point of action of C' while the tension force T' is determined from the placement of the tendons. The force is usually taken to act at the centroid of the tendon steel. Where both tendons and reinforcing bars are used in the same beam as tension steel, T' would be solved for each type of reinforcement and these two forces (acting at centroid of each type of steel) would be combined into a single total resultant, T'.

Strain at ultimate, Item 6, is based on test data. The ACI Code value for design, 0.003 in./in., is a lower-bound value from these data. Actually, the assumption of higher strain for crushing of concrete doesn't significantly change the ultimate moment calculated. Higher strain at ultimate would lead to greater deformation, thus the ACI Code value may be considered purposely conservative for safe design. Only a very lightly reinforced beam would fail by fracture of the steel prior to reaching crushing strain in the concrete at the extreme compressive fiber. As indicated by Item 7, we assume no other type of failure occurs; that is, this flexural analysis cannot assure adequate shear, bond, or anchorage strength since these must be checked separately.

The analysis procedure is carried out assuming two stages of behavior: first, the beam is elastic and uncracked; second, the beam is cracked and the actual

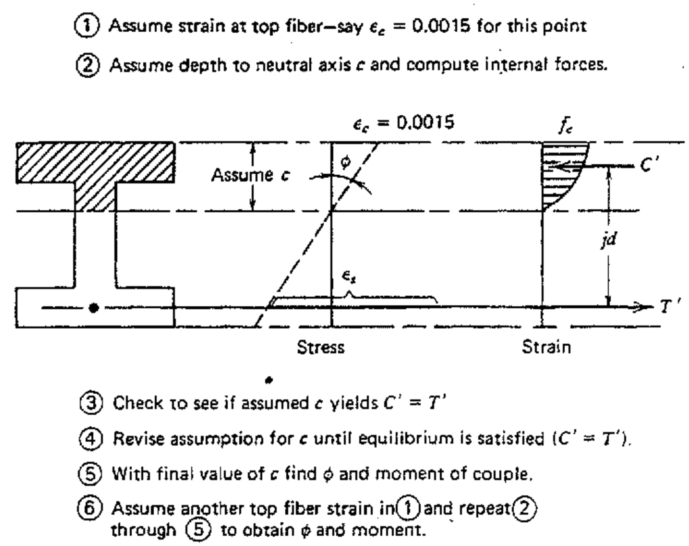

Fig. 5-24. Postcracking analysis for moment-curvature.

material properties are used for analysis of the cracked section response. The first stage is assumed elastic, but the second stage is inelastic following the response of the materials. Figure 5-24 shows the steps in the postcracking analysis. A point-to-point check is made for a series of assumed values for top fiber strain, the points collectively describing the moment-curvature relationship as shown in the numerical example, example 5-10.

EXAMPLE 5-10

The beam cross section of example 5-8 is to be analyzed to determine its moment-curvature relationship. The materials are normal weight concrete; $f'_c = 7000$ psi (48 N/mm²), limiting strain at ultimate = 0.003; 7-wire strand with $f_{pu} = 270$ ksi (1.862 N/mm²) specified. Use the *actual* curve for analysis, Fig. 5-25a, which has breaking strength of approximately 280 ksi (1,931 N/mm²) from typical test. (Figure 5-25b shows f_c vs. ϵ_c for concrete.)

Find points for moment, M, and curvature, ϕ, for each of these stages as moment is increased:

(a) Initial stage—zero applied moment, $f_{se} = 160$ ksi.
(b) Zero strain in concrete at level of steel.
(c) Cracking at $f_r = 7.5\sqrt{f'_c}$.
(d) Top fiber strain 0.001. } cracked section
(e) Top fiber strain 0.002. } cracked section
(f) Top fiber strain 0.003. } cracked section

Make a summary of results including the steel stress at each stage, and plot the M vs. ϕ curve.

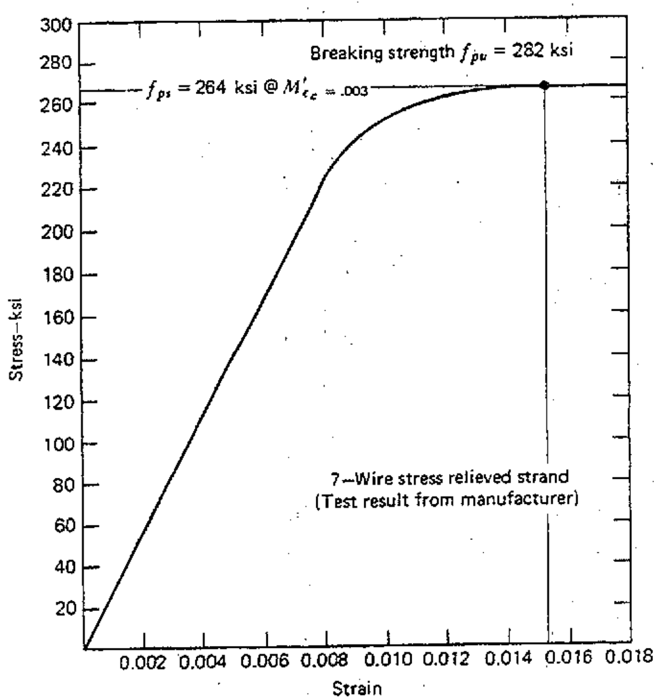

(*a*) Steel Stress-Strain Curve

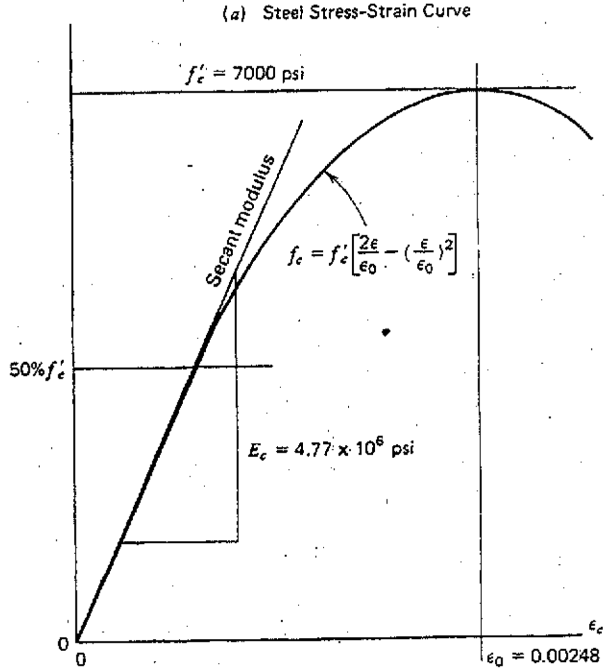

(*b*) Concrete Stress-Strain Curve

Fig. 5-25. Stress-strain curves for materials, example 5-10.

Solution (*a*) *Initial stage*: assume elastic beam may be analyzed for stresses in the concrete using gross section properties and $F = A_{ps} f_{se}$

Section properties: $A = 373$ in.^{2} (241×10^3 mm^2) $c = 18$ in. (457.2 mm)

(Fig. 5-17 shows cross-section dimensions)

$$I_x = 58{,}890 \text{ in.}^4\ (24.51 \times 10^9 \text{ mm}^4)\quad e = 13.5 \text{ in. } (342.9 \text{ mm})$$

$$S_x = 3272 \text{ in.}^3\ (53.62 \times 10^6 \text{ mm}^3)$$

$$F = (2.75)(160) = 440 \text{ k } (1957 \text{ kN})$$

$$E_c = 57{,}000\sqrt{f'_c} = 57{,}000\sqrt{7000} = 4.77 \times 10^6 \text{ psi } (32.89 \text{ kN/mm}^2)$$

Compute stress and corresponding strains in section due to $F = 440$ k (1957 kN) at $e = 13.5$ in. (342.9 mm).

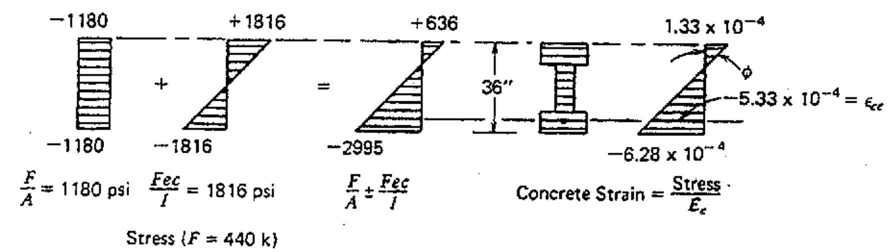

Fig. 5-26(*a*). Initial stage, example 5-10.

$$\phi = \text{curvature (slope of Fig. 5-26}(a)\text{ strain gradient)} = \frac{1.33 \times 10^{-4} + 6.28 \times 10^{-4}}{36}$$

$$\phi = -2.11 \times 10^{-5} \text{ rad/in. at } M = 0 \text{ (applied moment)}$$

Find $\qquad \epsilon_{se}$ = steel strain at $f_{se} = 160$ ksi (1103 N/mm^2)

$$\epsilon_{se} = \frac{160{,}000}{27.5 \times 10^6} = 5.82 \times 10^{-3}$$

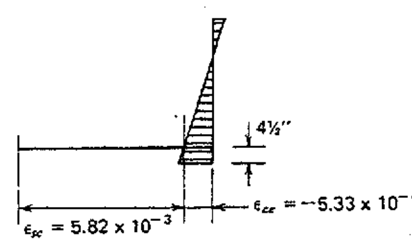

Fig. 5-26(*b*). Initial steel and concrete strains, example 5-10.

(*b*) *Zero strain in concrete at level of steel*: an applied moment which produces $\epsilon_{ce} = 5.33 \times 10^{-4}$ at the level of steel will cause the strain in the concrete to be zero as desired for this step. We note that the same change in strain will occur in the bonded steel, thus the steel strain will become

$$\epsilon_{ps} = \epsilon_{se} + \epsilon_{ce} = 5.82 \times 10^{-3} + 0.533 \times 10^{-3} = 6.35 \times 10^{-3}$$

$$f_{ps} = \epsilon_{ps} \times E_{ps} = 6.35 \times 10^{-3} \times 27.5 \times 10^{3} = 175 \text{ ksi } (1207 \text{ N/mm}^2)$$

$$F = (2.75)(175) = 481 \text{ k } (2139 \text{ kN})$$

Thus the effective stress increases from that in (*a*), and we can find the concrete stresses which result from this increased force as shown in Fig. 5-26(*c*).

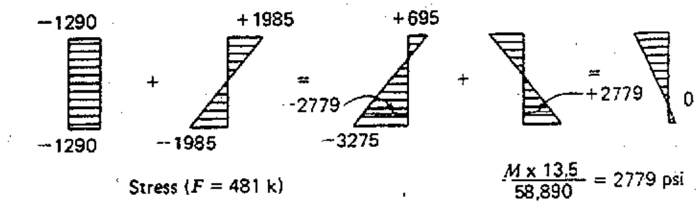

Fig. 5-26(c). Stresses for example 5-10 at stage (b).

Solving M from the stress to reduce to zero the combined stress (and strain) at level of steel as shown in Fig. 5-26(*c*) and using 2779 psi = 2.779 ksi:

$$M = \frac{2.779 \times 58{,}890}{13.5} = 12{,}120 \text{ in.-k } (1370 \text{ kN} - \text{m})$$

Complete the combined stress sketch with this M acting, and find corresponding strains (stress/E_c) to allow ϕ to be solved as shown in Fig. 5-26(*d*).

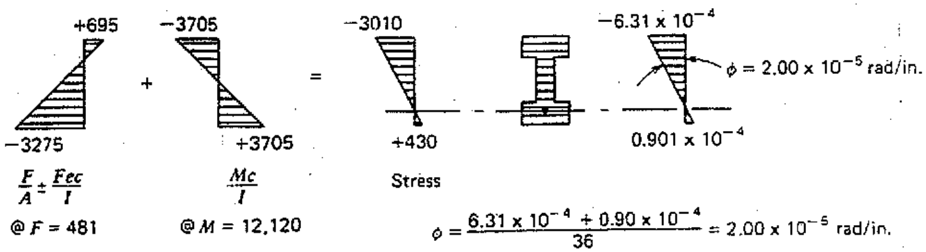

Fig. 5-26(d). Solving curvature at stage (b), example 5-10.

From these calculations we have determined a second point in the elastic range of behavior:

$$M = 12{,}120 \text{ in.-k } (1{,}370 \text{ kN} - \text{m}).$$

$$\phi = +2.00 \times 10^{-5}$$

(*c*) The two previous points will be used to establish the linear elastic response of the moment-curvature relationship, but we wish now to estimate the cracking moment which is the endpoint for this uncracked section analysis. M_{cr} is associated with $f_r = 7.5\sqrt{f_c'}$, the modulus of rupture for concrete.

$$f_r = 7.5\sqrt{7000} = 627 \text{ psi } (4.32 \text{ N/mm}^2)$$

Since the bottom fiber stress has 430 psi (2.96 N/mm²) tension stress at stage (*b*) above, we can see that it will require only a rather small moment additional to pick up the additional tension stress

$$627 - 430 = 197 \text{ psi}$$
$$= 0.197 \text{ ksi } (1.36 \text{ N/mm}^2)$$

$$\Delta M = \frac{\Delta f I}{c} = \frac{(0.197)(58{,}890)}{18} = 645 \text{ in.-k } (73 \text{ kN} - \text{m})$$

$$M_{cr} = 12{,}120 + 645 = 12{,}765 \text{ in.-k } (1443 \text{ kN} - \text{m})$$

The very slight additional tension strain in the steel which accompanies this moment could be neglected. We can determine it rather easily however since

$$\Delta f_{ps} = n\frac{\Delta M y}{I}$$

where y = distance to c.g.s. = 13.5 in.

$$\Delta f_{ps} = \frac{27.5}{4.77} \times \frac{645 \times 13.5}{58{,}890} = 0.85 \text{ ksi } (5.86 \text{ N/mm}^2)$$

The steel stress at M_{cr} is

$$f_{ps} = 175 + 0.85 \cong 176 \text{ ksi } (1214 \text{ N/mm}^2)$$

We can also evaluate the additional curvature, which must be associated with the additional 197 psi (1.36 N/mm²) extreme fiber stress, Fig. 5-26(*e*), and obtain the cracking curvature, ϕ_{cr}.

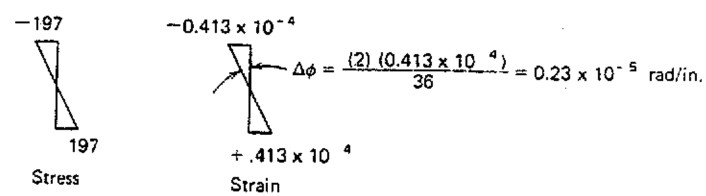

ϕ_{cr} = Stage b curvature + $\Delta\phi$

$\phi_{cr} = 2.00 \times 10^{-5} + 0.23 \times 10^{-5} = 2.23 \times 10^{-5}$ rad/in.

Fig. 5-26(e). Additional curvature to cause cracking, example 5-10.

(*d*) The top fiber strain at cracking is the combination of the results from (*b*) and (*c*):

$$\epsilon_c = -6.31 \times 10^{-4} - 0.413 \times 10^{-4} = -6.72 \times 10^{-4}$$

$$\epsilon_c = -0.000672 \text{ in/in.} < -0.001 \text{ in./in.}$$

We know that the cracked section analysis is valid for the next point asked for where $\epsilon_c = 0.001$.

The step-by-step procedure of Fig. 5-24 will now be followed for $\epsilon_c = 0.001$ (top fiber strain). The expression from Fig. 5-21(c) for resultant compression force and its point of action will be used in this solution. The stress-strain curve for the steel, Fig. 5-25, is used as well as the prior strain in the steel at stage (b) when zero strain existed in the concrete at level of steel. From (b) we know that

$$\epsilon_{se} + \epsilon_{ce} = 6.35 \times 10^{-3}$$

The first trial-neutral axis assumed 12 in. (304.8 mm) below the top fiber as shown in Fig. 5-26(f).

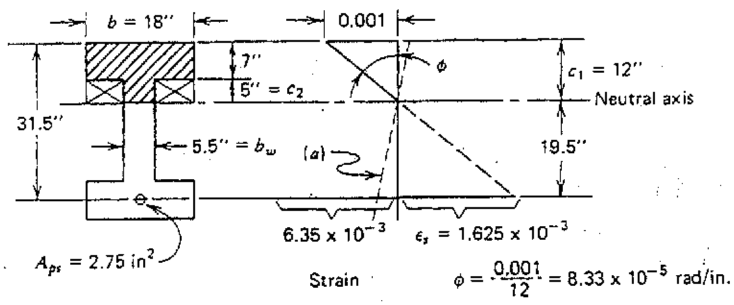

Fig. 5-26(f). First trial stage (d), example 5-10.

From the sketch above we note the neutral axis falls in the web, thus the compression zone is not rectangular as assumed in the derivation of the expression for resultant compression in Fig. 5-21(c). We will first assume the width $b = 18$ in. (457.2 mm) extends to the neutral axis as shown on the sketch and solve the resultant compressive force C_1. Next we will correct this by using the width $(b - b_w)$ for the 5 in. (127 mm) above the neutral axis as shown blocked out on the sketch. This C_2 force will be given a negative sign, and the resultant compression C_c will be the algebraic sum of C_1 and C_2.

$$C_c = bc^2 f_c' \frac{\phi}{\epsilon_0}\left[1 - \frac{\phi c}{3\epsilon_0}\right] \tag{5-29}$$

where $\epsilon_0 = 0.00248 = 2.48 \times 10^{-3}$ in./in. from 5-25(b) gives secant modulus of elasticity assumed in previous parts.

$$C_{c_1} = (18)(12)^2(7000)\frac{8.33\times10^{-5}}{2.48\times10^{-3}}\left[1 - \frac{(8.33\times10^{-5})(12)}{(3)(2.48\times10^{-3})}\right] \tag{5-29}$$

$C_{c_1} = 527{,}500$ lb (2346 kN)

Using $b = 18 - 5.5 = 12.5$ in. (317.5 mm) for C_{c_2} correction:

$$C_{c_2} = -(12.5)(5)^2(7000)\left(\frac{8.33\times10^{-5}}{2.48\times10^{-3}}\right)\left[1 - \frac{(8.33\times10^{-5})(5)}{(3)(2.48\times10^{-3})}\right] \tag{5-29}$$

$C_{c_2} = -69{,}360$ lb (-308.5 kN)

$C_c = 527{,}500 - 69{,}360 = 458{,}140$ lb $= 458$ k (2,037 kN)

From Fig. 5.26(f) find strain in the prestressing steel

$$\epsilon_{ps} = 6.35\times10^{-3} + 1.625\times10^{-3} = 7.98\times10^{-3}$$

From Fig. 5-25 we determine stress corresponding to this strain to be $f_{ps} = 218$ ksi (1503 N/mm²). For $A_{ps} = 2.75$ in.² (1774 mm²) the tension is

$$T = (2.75)(218) = 600 \text{ k } (2669 \text{ kN}) > C_c = 458 \text{ k } (2037 \text{ kN})$$

The neutral axis is too high, resulting in a steel strain which is too high, making $T > C_c$. For the second trial make the assumed distance to the neutral axis larger.

Second trial—neutral axis assumed 16.5 in. (419.1 mm) below top fiber as shown in Fig. 5-26(g).

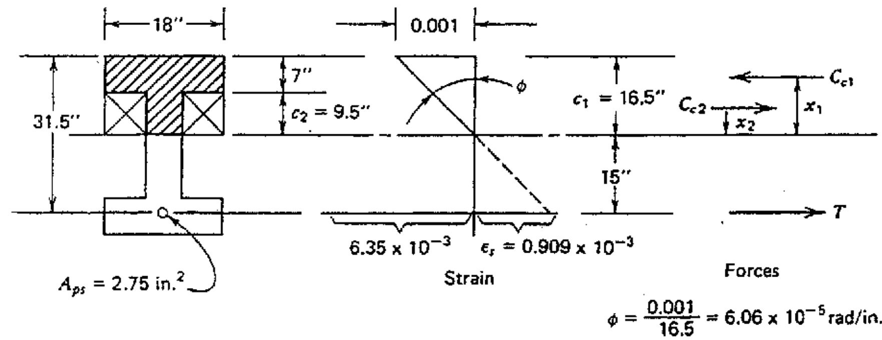

Fig. 5-26(g). Second trial stage (d), example 5-10.

$$C_{c_1} = (18)(16.5)^2(7000)\left(\frac{6.06\times10^{-5}}{2.48\times10^{-3}}\right)\left[1 - \frac{(6.06\times10^{-5})(16.5)}{(3)(2.48\times10^{-3})}\right] \tag{5-29}$$

$C_{c_1} = 725{,}700$ lb (3228 kN)

$$C_{c_2} = -(12.5)(9.5)^2(7000)\left(\frac{6.06\times10^{-5}}{2.48\times10^{-3}}\right)\left[1 - \frac{(6.06\times10^{-5})(9.5)}{(3)(2.48\times10^{-3})}\right] \tag{5-29}$$

$C_{c_2} = -178{,}060$ lb (-792 kN)

$C_c = 725{,}700 - 178{,}060 = 547{,}640$ lb $= 548$ k (2436 kN)

From Fig. 5-26(g) find strain in prestressing steel

$$\epsilon_{ps} = 6.35\times10^{-3} + 0.909\times10^{-3} = 7.26\times10^{-3}$$

From Fig. 5-25 we determine the steel stress, f_{ps}, corresponding to this strain to be 200 ksi (1379 N/mm²) and $A_{ps} = 2.75$ in.² (1774 mm²) is known, thus

$$T = (2.75)(200) = 550 \text{ k } (2{,}225 \text{ kN}) \approx 548 \text{ k } (2436 \text{ kN}) = C_c$$

Referring to Fig. 5-26(g) and using expression (5-30) from Fig. 5-21(c) to locate resultant C_c forces:

$$\bar{x}=c\left[\frac{8\epsilon_0-3\phi c}{12\epsilon_0-4\phi c}\right] \text{ measured from neutral axis} \tag{5-30}$$

$$\bar{x}_1=16.5\left[\frac{(8)(2.48\times10^{-3})-(3)(6.06\times10^{-5})(16.5)}{(12)(2.48\times10^{-3})-(4)(6.06\times10^{-5})(16.5)}\right]=10.8 \text{ in. } (274 \text{ mm})$$

$$\bar{x}_2=9.5\left[\frac{(8)(2.48\times10^{-3})-(3)(6.06\times10^{-5})(9.5)}{(12)(2.48\times10^{-3})-(4)(6.06\times10^{-5})(9.5)}\right]=6.25 \text{ in. } (159 \text{ mm})$$

Summing moments about the tension steel location

$$M=C_{c1}(15+\bar{x}_1)-C_{c_2}(15+\bar{x}_2)$$
$$=(725.7)(15+10.8)-(178.1)(15+6.25)$$
$$M=14{,}940 \text{ in.-k } (1{,}688 \text{ kN}-\text{m}) \text{ at } \phi=6.06\times10^{-5}$$

(e) With top fiber strain $=0.002$ the solution is carried out as above. The results are

$c=10$ in. (254 mm)—top fiber to neutral axis

$C_c=T=688$ k (3060 kN)

$f_{ps}=250$ ksi (1724 N/mm^2)

$M=19{,}200$ in.-k. (2170 kN$-$m)

$\phi=20.0\times10^{-5}$ rad/in.

(f) With top fiber strain $=0.003$ the solution will be shown. This is the ultimate moment corresponding to the limiting strain specified by the ACI Code.

Try $c=8$ in. (203.2 mm) with top fiber strain 0.003 as shown in Fig. 5-26(h):

$$C_{c_1}=(18)(8)^2(7000)\left(\frac{37.5\times10^{-5}}{2.48\times10^{-3}}\right)\left[1-\frac{(3.75\times10^{-5})(8)}{(3)(2.48\times10^{-3})}\right] \tag{5-29}$$

$$C_{c_1}=727{,}000 \text{ lb } (3234 \text{ kN})$$

$$C_{c_2}=-(12.5)(1)^2(7000)\left(\frac{37.5\times10^{-5}}{2.48\times10^{-3}}\right)\left[1-\frac{(3.75\times10^{-5})(1)}{(3)(2.48\times10^{-3})}\right] \tag{5-29}$$

$$C_{c_2}=-12{,}500 \text{ lb } (-55.6 \text{ kN})$$

$$C_c=727{,}000-12{,}500=714{,}500 \text{ lb}=715 \text{ k } (3178 \text{ kN})$$

From Fig. 5-26(h) find strain in the prestressing steel

$$\epsilon_{ps}=6.35\times10^{-3}+8.81\times10^{-3}=15.16\times10^{-3}$$

From Fig. 5-25 we find the stress corresponding to this strain

$$f_{ps}=264 \text{ ksi } (1820 \text{ N/mm}^2)$$

$$T=(2.75)(264)=726 \text{ k } (3{,}229 \text{ kN}) \text{ vs. } C_c=715 \text{ k } (3178 \text{ kN})$$

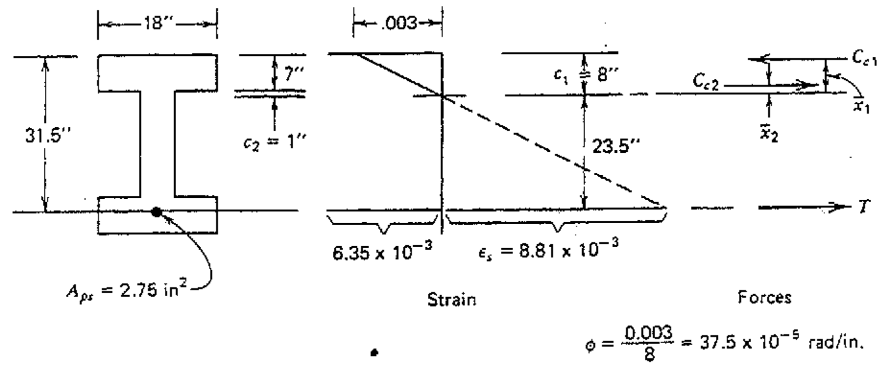

Fig. 5-26(h). Stage (f), example 5-10.

This is acceptable within 1.5%.

$$\bar{x}_1=8\left[\frac{(8)(2.48\times10^{-3})-(3)(37.5\times10^{-5})(8)}{(12)(2.48\times10^{-3})-(4)(37.5\times10^{-5})(8)}\right]$$

$$\bar{x}_1=4.86 \text{ in. } (123.4 \text{ mm}) \tag{5-30}$$

$$\bar{x}_2=1\left[\frac{(1)(2.48\times10^{-3})-(3)(37.5\times10^{-5})(1)}{(12)(2.48\times10^{-3})-(4)(37.5\times10^{-5})(1)}\right]$$

$$\bar{x}_2=0.66 \text{ in. } (16.8 \text{ mm}) \tag{5-30}$$

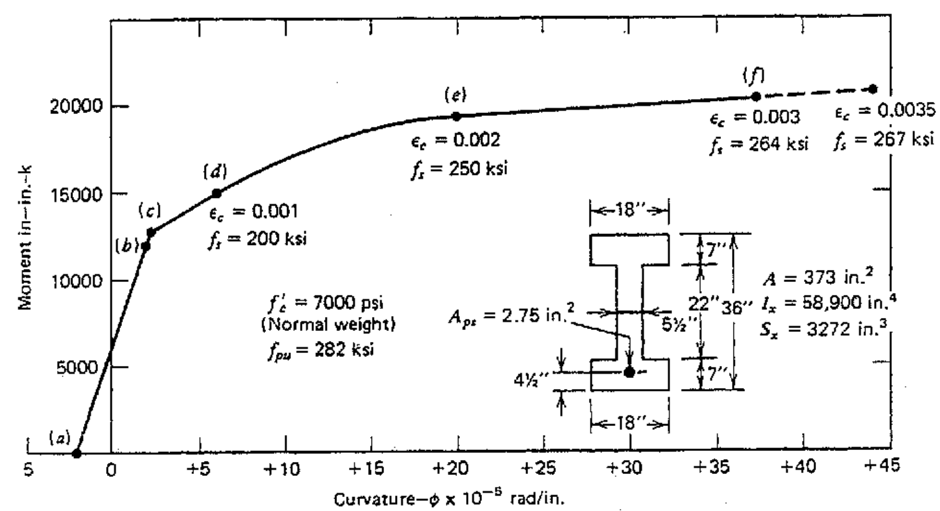

Fig. 5-27. Moment-curvature results, example 5-10.

Summing moments about the tension steel:

$$M' = (727)(23.5+4.86) - (12.5)(23.5+0.66)$$

$$M' = 20{,}320 \text{ in.-k } (2296 \text{ kN}-\text{m}) \text{ at } \phi = 37.5\times10^{-5}$$

Summary of results for example 5-10 (plotted Fig. 5-27):

Stage	Moment (in.-k)	Curvature (rad/in.)	Steel Stress (ksi)
(a)	0	-2.11×10^{-5}	160
(b)	12,120	$+2.00\times10^{-5}$	175
(c)	12,765	$+2.23\times10^{-5}$	176
(d)	14,940	$+6.06\times10^{-5}$	200
(e)	19,200	$+20.0\times10^{-5}$	250
(f)	20,320	$+37.5\times10^{-5}$	264

The use of the actual test curve results in $M' = 20{,}320$ in.-k (2,296 kN − m) as the ultimate moment in example 5-10. We must make two observations in order to compare this result with the ACI Code M_u for this same section in example 5-8. First, the estimate in example 5-8 was made with $f_{pu} = 270$ ksi (1862 N/mm^2), the guaranteed strength rather than $f_{pu} = 282$ ksi (1944 N/mm^2), the actual strength in example 5-10 (Fig. 5-25, stress-strain curve). Second, the M_u in example 5-8 was that for ultimate design moment under the ACI Code, $M_u = \phi M' = 0.9M'$. We can make corrections for both factors and then compare M_u values.

We will estimate that the ultimate moment is increased in proportion to f_{pu} for example 5-10. Making this correction we have

$$M' = \left(\frac{270}{282}\right)(20{,}320) = 19{,}460 \text{ in.-k } (2199 \text{ kN}-\text{m})$$

$$M_u = (0.9)(19{,}460) = 17{,}510 \text{ in.-k } (1979 \text{ kN}-\text{m}) \text{ vs. } 17{,}220 \text{ in.-k } (1944 \text{ kN}-\text{m})$$

(example 5-10) (example 5-8)

This excellent agreement indicates that the ACI Code estimate is certainly adequate for analysis when performing strength design.

The moment-curvature analysis allows the total range of performance to be examined, and the last point on Fig. 5-27 is the ultimate moment. We will find this total curve useful later in making estimates of ultimate deflection. It is generally true, however, that the load-deflection curve for a beam will have the same form as the $M-\phi$ curve. Thus, the curve of Fig. 5-27 indicates ductile behavior which we want in structural design. The curvature at the ultimate moment is much larger than that at cracking, and most designs of prestressed concrete beams limit stress at service load to keep the beam uncracked.

Another observation from the moment vs. curvature curve of Fig. 5-27 is that the ratio of ultimate moment to cracking moment is 1.59. The ACI Code requires that this ratio be at least 1.2 to insure that a beam will not have the possibility of collapse at the instant of cracking. Increase in strength after cracking as observed in Fig. 5-27 is the behavior we desire in the design of prestressed concrete beams.

The versatility and reliability of the moment-curvature analysis are apparent in the observed test results shown compared to calculated response shown in Fig. 5-28. Note that this curve is for a member with both prestressed strands and unstressed reinforcing bars. The procedure for finding moment and corresponding curvature for points defining the M vs. ϕ curve for this beam would be done in the step-by-step manner described in example 5-10.

The only special consideration here which was not a part of the previous example is illustrated by Fig. 5-29, which shows the internal forces. Note that the two types of steel are handled separately, and the difference in their strain histories is taken into account in the analysis. The force T'_{ps} in the prestressed strands would be calculated from the area A_{ps} for the strands and the stress for the strand material which corresponds to the total strain $(\epsilon_{ce} + \epsilon_{se} + \epsilon_{si})$, Fig.

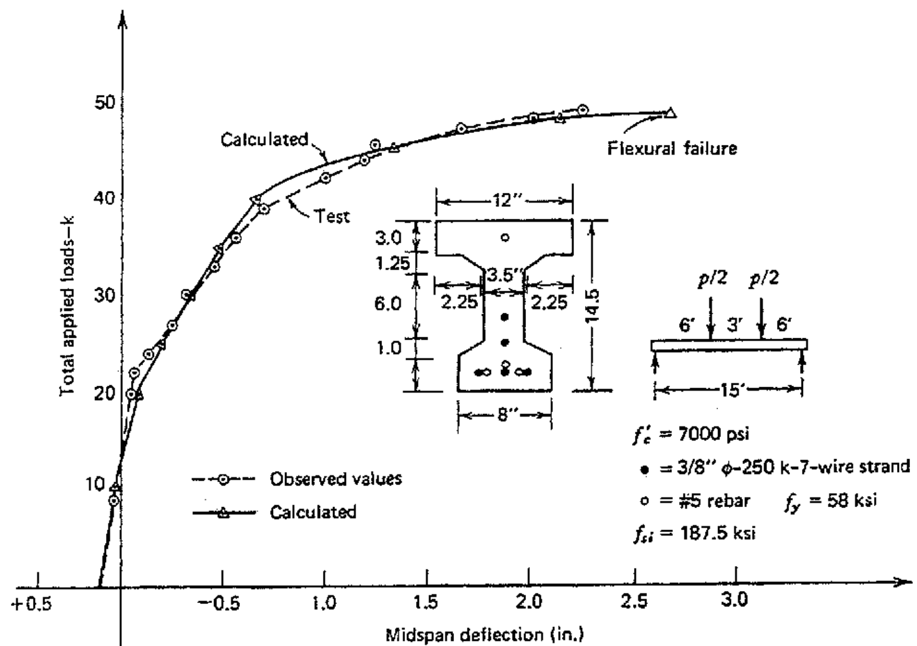

Fig. 5-28. Comparison of load-deflection observed (test) and calculated (analysis using $M-\phi$ curve).

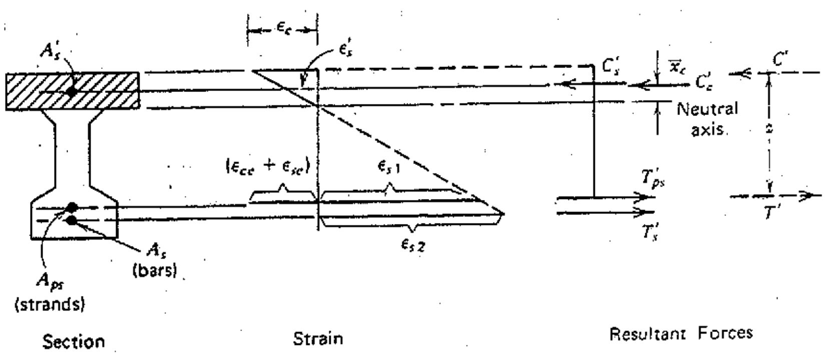

Fig. 5-29. Forces acting for beam of Fig. 5-28.

5-29. The force T_s' in the unstressed bars, A_s, would be calculated from the area A_s and the stress for the reinforcing bar material which corresponds to the strain ϵ_{s_2}, Fig. 5-29. These two tension forces combine to form the total resultant T', which must be equal to the total resultant compression C', and the moment M' would be $M'=T'z=C'z$.

The compression force C_c' in the concrete would be computed for an assumed neutral axis position and top fiber strain, ϵ_c, as was done in example 5-10. If the neutral axis were in the web, this calculation might be done in two parts as shown previously with C_c' being the resultant compression force acting at a distance $\bar{x}_c$ above the neutral axis, Fig. 5-29. The compression steel reinforcing bar, A_s', has a stress corresponding to ϵ_s' from the material stress-strain curve; thus the force C_s' may be solved. The total compression C' is the resultant of the steel and concrete compressive forces, Fig. 5-29.

Fig. 5-28 shows the load-deflection response which has the same form as the $M-\phi$ relationship for the cross section. The deflection for load levels after cracking must be computed by utilizing the known moment diagram for the simple beam together with the $M-\phi$ relationship solved by analysis of the cross section. Figure 5-30 shows the changing form of the distribution of curvature along the span at various load levels. As load approaches ultimate, note that the ultimate curvature, ϕ, at midspan is much larger than the curvature at this section at cracking. As shown by the load-deflection curve of Fig. 5-28, the deflection at ultimate is much larger than at cracking. The deflection is calculated from the distribution of curvature along the span, shown in Fig. 5-30 as the ϕ diagram. We must sum the moment about A of area under the diagram between A and B (shaded in Fig. 5-30) to obtain the deflection at B. Note that this calculation would reflect the large contribution to deflection which results from the large curvatures which develop in the middle portion of the span with flexural cracking. The end regions of the beam remain uncracked in flexure (Fig. 5-30) since the moment is less than the cracking moment in these regions, and

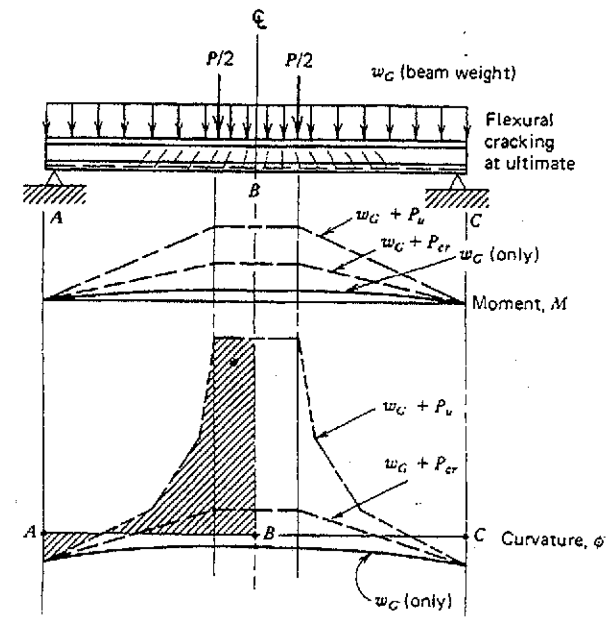

Fig. 5-30. Moment and curvature at various load levels.

they contribute insignificantly to the deflection after extensive cracking has developed.

More will be said about deflections in Chapter 8, but this tie between curvature along the span and the resulting deflection should be thought of as a part of analysis for flexure. As discussed here, the flexural behavior of a simple beam with bonded reinforcement may be analyzed for the whole range of applied load. This analysis may be coded for the computer, but only a few points from hand calculation can give reasonable accuracy. Normally, we want the character of the response and not an exact prediction of ultimate deflection.

5-8 Ultimate Moment—Unbonded Beams

An accurate calculation for the ultimate strength of unbonded beams is more difficult than for that of bonded ones, because the stress in the steel at rupture of the beam cannot be closely computed. Also there have not been sufficient data on the ultimate strength of unbonded beams to establish definitely a reliable method of computation. It is agreed, however, that unbonded beams are weaker than the corresponding bonded ones in their ultimate strength, the difference being placed at 10–30%.

Explanations can be offered for the lower strength of unbonded beams. First, since the tendon is free to slip, the strain in a tendon is more or less equalized along its length, and the strain at the critical section is lessened. Hence the stress in the tendon is increased only slowly so that, when the crushing strain has been reached in the concrete, stress in the steel is often far below its ultimate strength. When there are no cracks in the beam, stress in steel can be computed as in solution 2, example 5-6. As soon as part of the beam cracks or is stretched into the plastic range, the stress cannot be conveniently calculated. For the purpose of design, however, it may be possible to estimate the stress in the steel at the rupture of the beam and to compute the corresponding lever arm so as to approximate the ultimate resisting moment. Until further test data are available, such estimation may often err by 10–15%. Fortunately, unbonded beams are not often used where ultimate strength is a controlling factor, and they are generally designed for the working loads by the elastic theory rather than for the ultimate load.

Another reason for the lower ultimate strength of unbonded beams is the appearance of a few large cracks in the concrete instead of many small ones well distributed. Such wide cracks tend to concentrate the strains in the concrete at these sections, thus resulting in early failure.

Tests prove that the ultimate strength of unbonded beams can be materially increased by the addition of nonprestressed steel. Such increase is attributed to the resistance of the nonprestressed steel itself as well as to its effect in distributing and limiting the cracks in the concrete. This will be discussed in Chapter 11. The ACI Code requires minimum amounts of bonded reinforcement to assure that cracking will be distributed along the span rather than allowing only one or two cracks in the unbonded member at ultimate.

A general formula for f_{ps}, the stress in steel at ultimate load, in an unbonded beam is

$$f_{ps}=f_{se}+\Delta f_s$$

where f_{se} is the effective prestress in the steel, and Δf_s is the additional stress in the steel produced as a result of beam bending up to the ultimate load. Tests at the University of Illinois (Fig. 117, reference 6) showed Δf_s varying from about 10,000 to 80,000 psi (68.95–551.6 N/mm²); those at the Portland Cement Association showed Δf_s between 40,000 and 60,000 psi (275.8 and 413.7 N/mm²) (p. 615, reference 5). Limited tests at the University of California indicated Δf_s varying from 30,000 psi to 80,000 psi (206.85–551.6 N/mm²), with the higher values of Δf_s occurring for the curved tendons, where frictional force probably restricted the free slipping of the wires, and for the beams which had a sizable amount of nonprestressed steel. Test results from simple and continuous beams at the University of Texas at Austin and the University of Washington show similar results.

Tests on simple and continuous beams by Mattock[11,12] at the University of Washington resulted in the correlation of f_{ps} as shown in Fig. 5-31. The

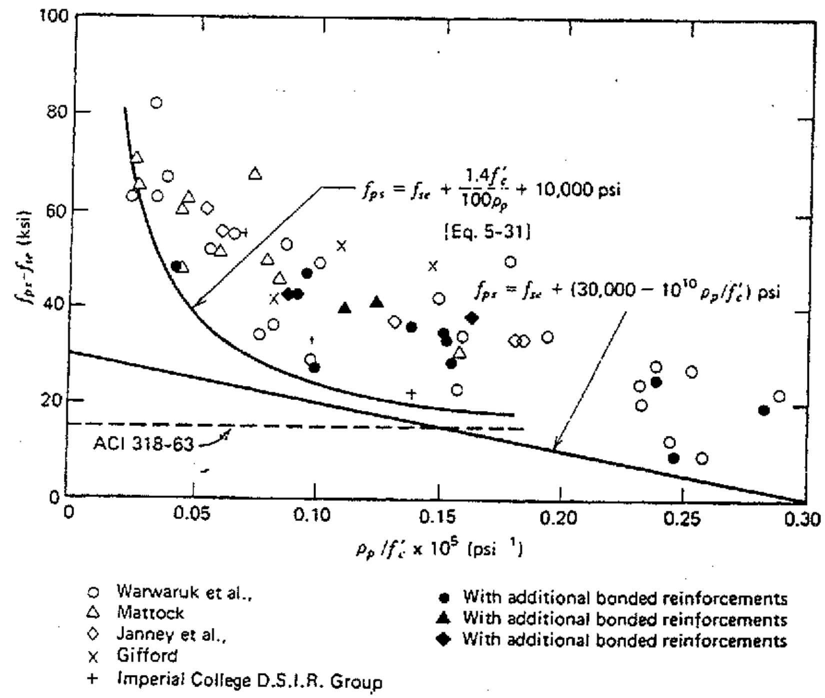

Fig. 5-31. Posttensioned beams without bond, increase in tendon stress during loading to ultimate.[12]

recommended equation for unbonded members which resulted from beam tests was as follows:

$$f_{ps}=f_{se}+10{,}000+\frac{1.4f'_c}{100\rho_p} \qquad (5\text{-}31)$$

The equation was slightly modified by ACI-ASCE Committee #423 to make it slightly more conservative, giving the following ACI Code equation:

$$f_{ps}=f_{se}+10{,}000+\frac{f'_c}{100\rho_p} \qquad (5\text{-}32)$$

where

$$f_{ps}\leqslant f_{py}$$

$$f_{ps}\leqslant f_{se}+60{,}000$$

In general, simple beams with unbonded tendons would be conservatively analyzed by this expression for f_{ps}. Shallow slabs (span/depth = 45) have been observed to develop slightly less than this f_{ps}, but the error is not significant. The geometry of the tendon layout enters into the elongation which will develop in the unbonded tendon. Almost no increase above f_{se} will result until after cracking. The Δf_s increase will develop as deflections become large, and equation 5-30 is adequate for analysis requiring the ultimate steel stress.

The analysis for ultimate moment M' for an unbonded beam would proceed as outlined above using the simplified ACI Code equation (5-32) for f_{ps}. The minimum bonded reinforcement which must be included for beams and one-way slabs to distribute cracking and also contribute to strength is given by the following expression:

$$A_s = 0.004A \qquad (5\text{-}33)$$

where

A = area of that part of the cross section between the flexural tension face and the center of gravity of the cross section

The steel which supplies this A_s acts at the specified yield point for the bars supplied, but not over 60,000 psi (414 N/mm²) may be used. Tests show that these bars will yield as assumed in analysis. Ample ductility is assured by the limitation on ω as required by the ACI Code, which assures that beams will be under-reinforced.

EXAMPLE 5-11

Assume the beam of Example 5-8 is provided with unbonded tendons but is otherwise the same as shown in Fig. 5-17. How much bonded reinforcement must be provided to satisfy ACI Code requirements? What is the estimated ultimate moment capacity of the section with $A_{ps} = 2.75$ in.² and minimum bonded reinforcement supplied with deformed bars having $f_y = 60$ ksi? Assume $f_{se} = 160$ ksi for the unbonded tendons, and $f_{py} = 230$ ksi; $f'_c = 7000$ psi as before. ($A_{ps} = 1.774$ mm², $f_y = 414$ N/mm², $f_{se} = 1{,}103$ N/mm², $f_{py} = 1{,}586$ N/mm², and $f'_c = 48$ N/mm²).

Solution

$$\rho_p = 0.00485 \text{ (same as example 5-8)}$$

for analysis of the beam use equation (5-31) here rather than the ACI Code equation (5-32) which is used for design.

$$f_{ps} = f_{se} + 10{,}000 + \frac{1.4 f'_c}{100\rho_p}$$

$$= 160{,}000 + 10{,}000 + \frac{(1.4)(7000)}{(100)(0.00485)}$$

$$f_{ps} = 160{,}000 + 10{,}000 + 20{,}200 = 190{,}200 \text{ psi } (1311 \text{ N/mm}^2) < f_{py}$$

$$= 230{,}000 \text{ psi } (1586 \text{ N/mm}^2)$$

$$\Delta f_s = 10{,}000 + 20{,}200 = 30{,}200 \text{ psi } (208 \text{ N/mm}^2) < 60{,}000 \text{ psi } (414 \text{ N/mm}^2)$$

Bonded reinforcement required by ACI Code:

$$A_s = 0.004A \qquad (5\text{-}33)$$

A = half of cross section area since neutral axis is at middepth of symmetrical I-shaped beam

$$A = (18-5.5)(7) + (5.5)(18) = 87.5 + 99 = 186.5 \text{ in.}^2 \ (120 \times 10^3 \text{ mm}^2)$$

$$A_s = (0.004)(186.5) = 0.75 \text{ in.}^2 \ (480 \text{ mm}^2) \qquad (5\text{-}33)$$

Use four #4 bars—$A_s = 0.80$ in.² (516 mm²)

For this problem assume this steel is placed 2 in. (50.8 mm) above bottom of section as shown in Fig. 5-32.

$$T'_p = f_{ps}A_{ps} = (190.2)(2.75) = 523 \text{ k } (2326 \text{ kN})$$

$$T'_s = f_y A_s = (60.0)(0.80) = 48 \text{ k } (213.5 \text{ kN})$$

$$T'(\text{total}) = 523 + 48 = 571 \text{ k } (2540 \text{ kN})$$

$$g = \frac{(523)(4.5) + (48)(2)}{571} = 4.29 \text{ in. } (109 \text{ mm})$$

$$T' = C' = 571 \text{ k} = (0.85)(f'_c)(b)(a)$$

$$a = \frac{571}{(0.85)(7.0)(18)} = 5.33 \text{ in. } (135 \text{ mm})$$

$$z = 36 - \frac{5.33}{2} - 4.29 = 29.04 \text{ in. } (738 \text{ mm})$$

$$M' = T'z = (571)(29.04) = 16{,}580 \text{ in.-k } (1.874 \text{ kN-m})$$

The ultimate moment is less than $M' = 19{,}100$ in.-k for the bonded beam of example 5-8 as anticipated. If the ACI Code were followed, the steel stress for the unbonded tendon from equation 5-30 is a little less ($f_{ps} = 184$ ksi), and this results in slightly smaller $M' = 16{,}130$ in.-k. In design this would be further reduced by the strength reduction

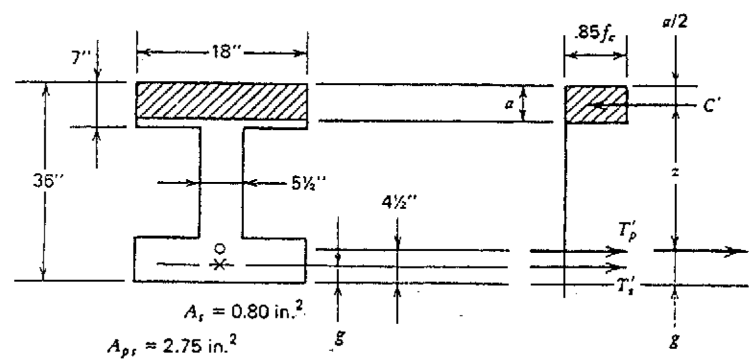

Fig. 5-32. Example 5-11.

factor $\phi = 0.9$. This beam would have $M_u = (0.9)\,(16{,}130) = 14{,}520$ in.-k following the ACI Code for design. Additional A_{ps} or A_s could be used to increase this to the $M_u = 17{,}200$ in.-k found for the bonded beam in example 5-8 if the design loads required this strength.

5-9 Composite Sections

In prestressed-concrete construction it is often advantageous to precast part of a section (either by pretensioning for by posttensioning), lift it to position, and cast the remainder of the section in place. The precast and cast-in-place portions thus act together (with stirrups if necessary) and form a composite section. Members of composite sections laid side by side may be eventually connected together by transverse prestressing, while such members laid end to end may be further prestressed longitudinally in order to attain continuity. These points will be discussed in later chapters. We shall describe here the basic method of analysis commonly employed for such composite sections.

Figure 5-33 shows a composite section at the midspan of simply supported beam, whose lower stem is precast and lifted into position with the top slab cast in place resting directly on the stem. If no temporary intermediate support is furnished, the weight of both the slab and the stem will be carried by the stem acting alone. After the slab concrete has hardened, the composite section will carry any live or dead load that may be added on to it.

In the same figure, stress distributions are shown for various stages of loading. These are discussed as follows.

(*a*) Owning to the initial prestress and the weight of the stem, there will be heavy compression in the lower fibers and possibly some small tension in the top fibers. The tensile force T in the steel and the compressive force C in the concrete form a resisting couple with a small lever arm between them.

(*b*) After losses have taken place in the prestress, the effective prestress together with the weight of the stem will result in a slightly lower compression in the bottom fibers and some small tension or compression in the top fibers. The C-T couple will act with a slightly greater lever arm.

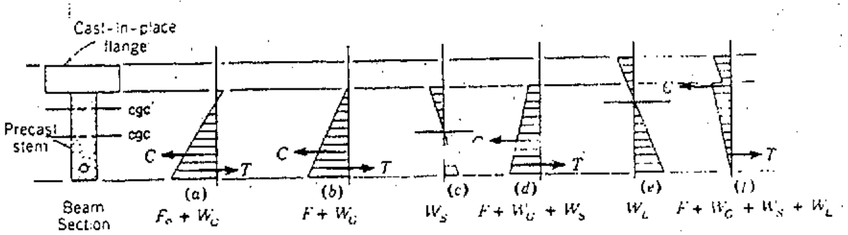

Fig. 5-33. Stress distribution for a composite section.

(*c*) Owning to the addition of the slab, its weight produces additional moment and stress as shown.

(*d*) Owning to the effective prestress plus the weight of the stem and slab, we can add (*b*) to (*c*) and a somewhat smaller compression is found to exist at the bottom fibers and some compression at the top fibers. The lever arm for the C-T couple further increases.

(*e*) Stresses resulting from live load moment are shown, the moment being resisted by the composite section.

(*f*) Adding (*d*) to (*e*), we have stress block as in (*f*), with slight tension or compression in the bottom fibers, but with high compressive stresses in the top fibers of the stem and the slab. The couple T and C now acts with an appreciable lever arm.

The above shows the stress distribution under working load conditions. For overloads, the stress distributions are shown in Fig. 5-34. For the load producing first cracks, it is assumed that the lower fibers reach a tensile stress equal to the modulus of rupture. This is obtained when the live-load stresses shown in Fig. 5-33(*e*) are big enough to result in a stress distribution as shown in Fig. 5-34(*a*), computed by the elastic theory.

Under the ultimate moment, however, the elastic theory is no longer valid. As an approximation, the ultimate resisting moment is best represented by a tensile force T' computed by the ACI equation for estimating f_{ps} acting with a compressive force C' supplied by the concrete. If failure in bond and shear is prevented, the ultimate strength of a composite section can be estimated by a method similar to that previously described for a simple prestressed section. It must be emphasized, however, that a composite section may fail in horizontal shear between the precast and the cast-in-place portions, unless proper stirrups or connectors are provided.

The above describes a simple case of composite action; there are many possible variations. First, the precast portion may be supported on falsework while the cast-in-place slab is being poured or placed, the falsework being removed only after the hardening of the slab concrete. This will permit the entire composite section to resist the moment produced by the weight of the slab. It is

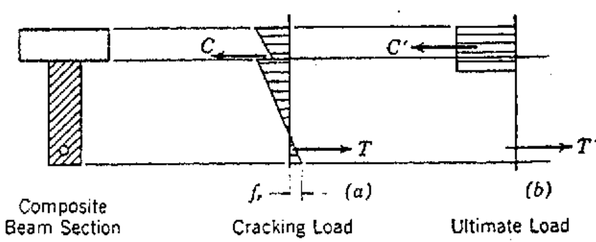

Fig. 5-34. Stress distributions for cracking and ultimate loads.

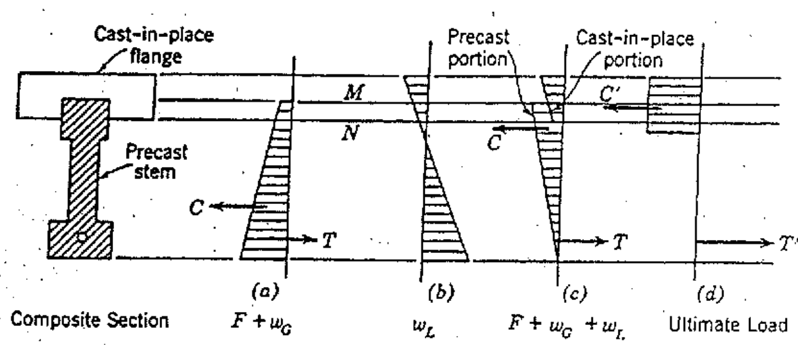

Fig. 5-35. Stress distribution for a special composite section.

also possible to prop up the falsework so that the stem will carry practically no moment by itself. Then the moments due to the weight of the stem will also be carried by the composite section. Since the composite section has a greater section modulus than the stem alone, the resulting stresses will be more favorable. The desirability of such methods depends on the cost of falsework for the particular structure.

Another variation happens when the cast-in-place slab overlaps with the precast portion as shown in Fig. 5-35. Here, the stresses in the concrete between levels *M* and *N* will follow two different variations, as shown in (*c*); one for the precast and another for the cast-in-place portion. At the ultimate range, however, they will all be stressed to the maximum and the difference will be hardly noticeable. Then the section can be analyzed as if it were a simple one, Fig. 5-35(*d*).

If the precast portion is only a small part of the whole section, it may be prestressed for direct tension only, or with a slight eccentricity of prestress. One method used in England (known as the Udall system), Fig. 5-36, employs both prestressed and nonprestressed wires in the groove of precast blocks, with the major top portion cast in place so as to be well bonded to the wires. For such a construction, high tension may exist in the bottom fibers of the cast-in-place

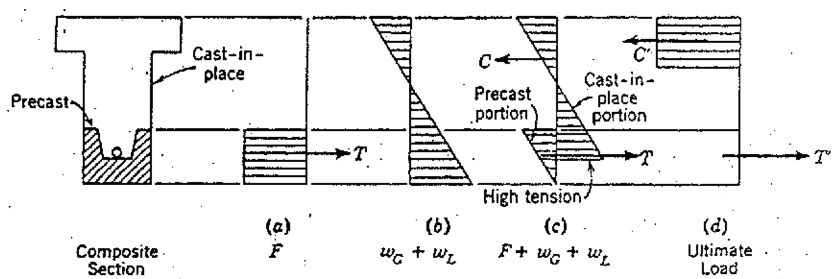

Fig. 5-36. Stress distribution for a special (Udall) composite section.

portion (*c*), resulting in cracks under working load. But the ultimate strength in flexure is not affected by the tensile stresses (*d*).

In other instances, the section is prestressed in two stages. Only part of the tendons are prestressed first in order to hold the stem together. The remaining tendons are prestressed after the slab has been cast and has hardened; otherwise the tendons may be partially prestressed first, to be fully prestressed later. If the process of retensioning is not too costly, this may result in an economical design. The stress distribution must be studied for the various stages, but the allowable stresses need not be the same as for an ordinary simple section. In certain instances, considerable tension may be permitted without adversely influencing performance of the member.

When differential shrinkage and creep between the precast and the in-place portions are considered, high stresses are obtained. The usual practice of neglecting such stresses can be justified on the grounds that the ultimate strength of the section is seldom affected by these stresses. However, the elastic behavior, such as camber and deflection, may be seriously modified. In practice, the in-place portion will have more shrinkage, since shrinkage of the precast portion has mostly taken place; but the precast portion will have more creep because it is usually under higher compression due to prestress. If the higher shrinkage in the in-place portion is just about balanced by the higher creep in the precast portion, it would be possible to neglect both. It often happens, however, that the shrinkage of the in-place portion is more serious, especially when the concrete has a high water-cement ratio. In this case the in-place concrete may crack, or the entire composite member may be forced to deflect downward.

EXAMPLE 5-12

The midspan section of a composite beam is shown in Fig. 5-37. The precast stem 12 in. by 36 in. (305 mm by 915 mm) deep is posttensioned with an initial force of 550 kips (2446 kN), Fig. 5-37(*a*). The effective prestress after losses is taken as 480 kips (2135 kN). Moment due to the weight of that precast section is 200 k-ft (271.2 kN-m) at midspan. After it is erected in place, the top slab of 6 in. by 36 in. (152 mm by 915 mm) wide is to be cast in place producing a moment of 100 k-ft (135.6 kN-m). After the slab concrete

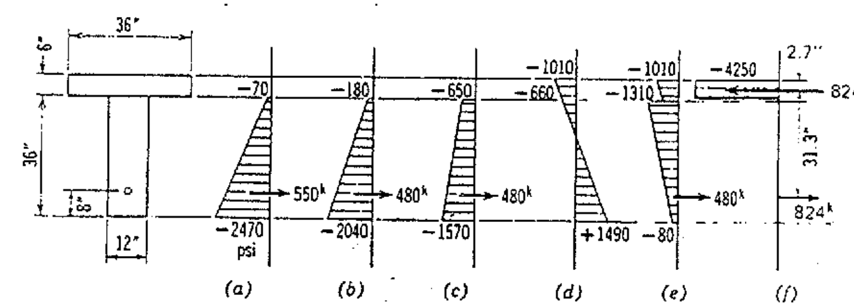

Fig. 5-37. Example 5-12.

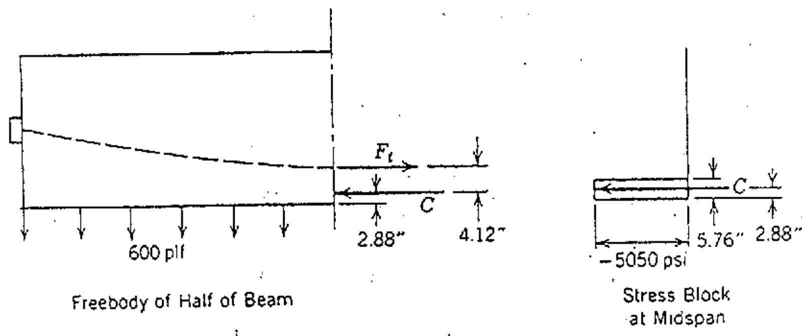

Fig. 5-40. Example 5-15.

EXAMPLE 5-15

Assuming the beam in example 5-15 is picked up suddenly at midspan so that an impact factor of 100% is considered, compute the maximum stress: $f'_c = 5000$ psi (34 N/mm²).

Solution The external moment will be doubled as a result of 100% impact, thus,

$$-M = 2 \times 2.06 \text{ in.} = 4.12 \text{ in. } (104.6 \text{ mm})$$

or located 2.88 in. (73.2 mm) above the bottom fiber. A triangular stress block will yield a high maximum stress of $2 \times 350{,}000/(8.64 \times 12) = 6750$ psi (46.54 N/mm²). Assuming a rectangular stress block, we have, Fig. 5-40,

$$\frac{350{,}000}{5.76 \times 12} = 5050 \text{ psi } (34.82 \text{ N/mm}^2) > 0.85 \times 5{,}000 = 4250 \text{ psi } (29.30 \text{ N/mm}^2)$$

Thus the beam would fail when picked up suddenly by a midspan pickup point. Note that trapezoidal stress block, using Jensen's theory, will give a more accurate answer,[13] but will not be attempted here as it is clear from the calculation above that the midspan pickup point exceeds the stress which the concrete could carry with $f'_c = 5000$ psi (34 N/mm²).

We would revise the pickup arrangement to use two points equidistant from midspan to avoid any possibility of damage to the beam during handling.

The three foregoing examples illustrate stress distributions in beams at transfer before cracking, after cracking, and at ultimate. The permissible stress values both in tension and in compression will depend on many factors, such as the shape of the section, the magnitude and location of the prestress, the chances of misplacement of the tendons, the probability of adverse moments, and the serious ness of cracking. Values specified in the ACI Code may be used as a reference.

References

1. G. L. Rogers, "Validity of Certain Assumptions in the Mechanics of Prestressed Concrete," *J. Am. Conc. Inst.*, December 1953 (*Proc.*, Vol. 49), pp. 317–330.
2. *International Federation of Prestressing, Preliminary Publications*, First International Congress, London, October 1953.

3. G. S. Ramaswamy and S. K. Narayana, "The Ultimate Flexural Strength of Posttensioned Grouted Rectangular Beams," *Papers, Third Congress of the International Federation of Prestressing*, Berlin, 1958.
4. D. F. Billet and J. H. Appleton, "Flexural Strength of Prestressed Concrete Beams," *J. Am. Conc. Inst.*, June 1954 (*Proc.*, Vol. 50), pp. 837–854.
5. J. R. Janney, E. Hognestad, and D. McHenry, "Ultimate Flexural Strength of Prestressed and Conventionally Reinforced Concrete Beams," *J. Am. Conc. Inst.*, February 1956 (*Proc.* Vol. 52), pp. 601–620.
6. J. Warwaruk, M. A. Sozen, C. P. Siess, "Strength and Behavior in Flexure of Prestressed Concrete Beams," Engineering Experiment Station *Bull. No. 464*, University of Illinois, 1962.
7. E. Hognestad, H. W. Hanson, and D. McHenry, "Concrete Stress Distribution in Ultimate Strength Design," *J. Am. Conc. Inst.*, December 1955 (*Proc.* Vol. 52), pp. 455–479.
8. "Tentative Recommendations for Prestressed Concrete," *J. Am. Conc. Inst.*, January 1958 (*Proc.* Vol. 54), pp. 545–578.
9. N. Burns, "Moment-Curvature Relationships for Partially Prestressed Concrete Beams," *J. Prestressed Conc. Inst.*, Vol. 9 No. 1, February 1964, pp. 52–63.
10. N. H. Burns, and C. P. Siess, "Load-Deformation Characteristics of Beam-Column Connections in Reinforced Concrete," Civil Engineering Studies, Structural Research Series No. 234, University of Illinois, January 1962.
11. Jun, Yamazaki, Basil T. Kattula, and Alan H. Mattock, "A Comparison of the Behavior of Posttensioned Prestressed Concrete Beams With and Without Bond," *Report* SM69-3, University of Washington, College of Engineering, Structures and Mechanics, December 1969, 94 pp.
12. Alan H. Mattock, Jun Yamazaki, and Basil T. Kattula, "Comparative Study of Prestressed Concrete Beams, With and Without Bond," *J. Am. Conc. Inst.* (*Proc.* Vol. 68) February 1971, pp. 116–125.
13. A. C. Scordelis, T. Y. Lin, and H. R. May, "Flexural Strength of Prestressed Concrete Beams at Transfer," *Proceedings World Conference on Prestressed Concrete*, San Francisco, 1957.